# Electron and neutrino scattering in the QE (and dip) region

Noemi Rocco

UNIVERSITY OF SURREY

‘Fundamental Physics with Electroweak Probes of Light Nuclei’ (INT-18-2a)
June 12 - July 13, 2018

Based on:

- NR, A. Lovato, and O. Benhar, Phys. Rev. Lett. **116**, 192501
- NR, A. Lovato, L. Alvarez-Ruso, A. Lovato, and J. Nieves, Phys. Rev. C **96**, 015504 (2017)
- NR, W. Leidemann, A. Lovato, G. Orlandini, Phys.Rev. C **97**, 055501 (2018)
- NR, C. Barbieri, arXiv:1803.00825

# Motivations

• In electron- scattering experiments the nucleus is mostly seen as a target, as the kinematic of the probe is completely known.

• The first generation of (e,e'p) data in the early 1960s not only established the validity of the nuclear shell model but alse showed its limitations

• More recent measurements, allowed to unveil detailed features of the nuclear wave function, including its high-momentum components.

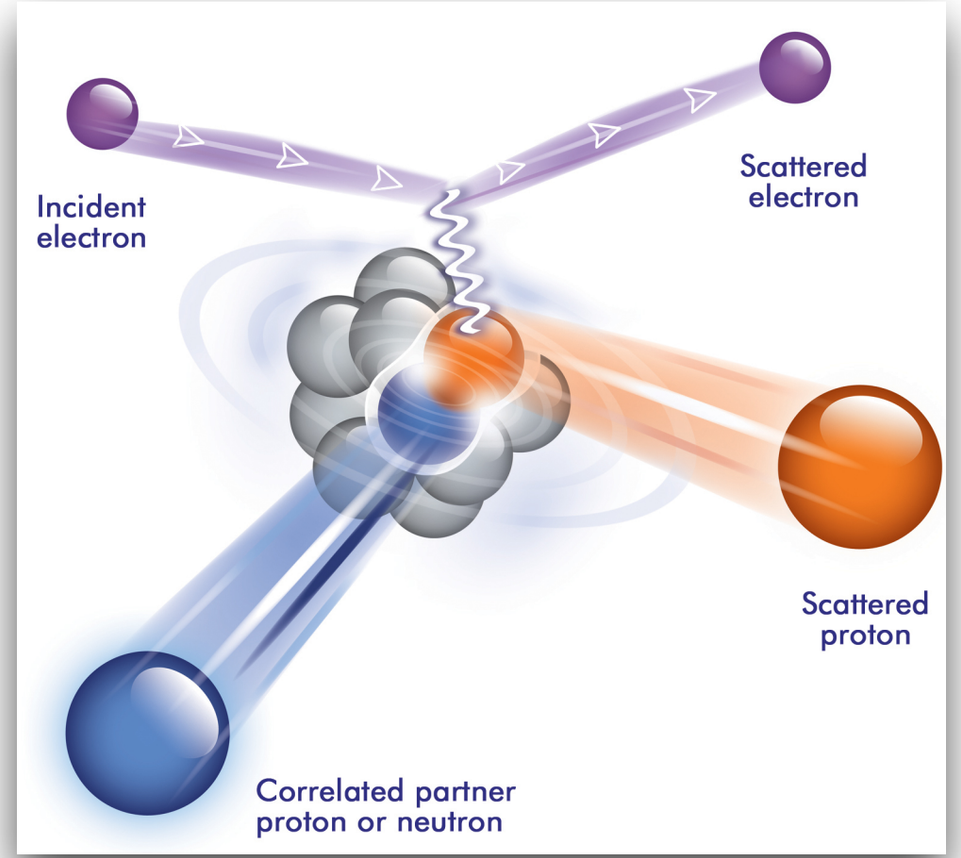


Subedi et al., Science 320, 1476 (2008)

• Developing a coherent picture of the electroweak response is also critical for the interpretation of neutrino scattering experiments, such as the Deep Underground Neutrino Experiment

# Electron-nucleus scattering

Schematic representation of the inclusive cross section as a function of the energy loss.

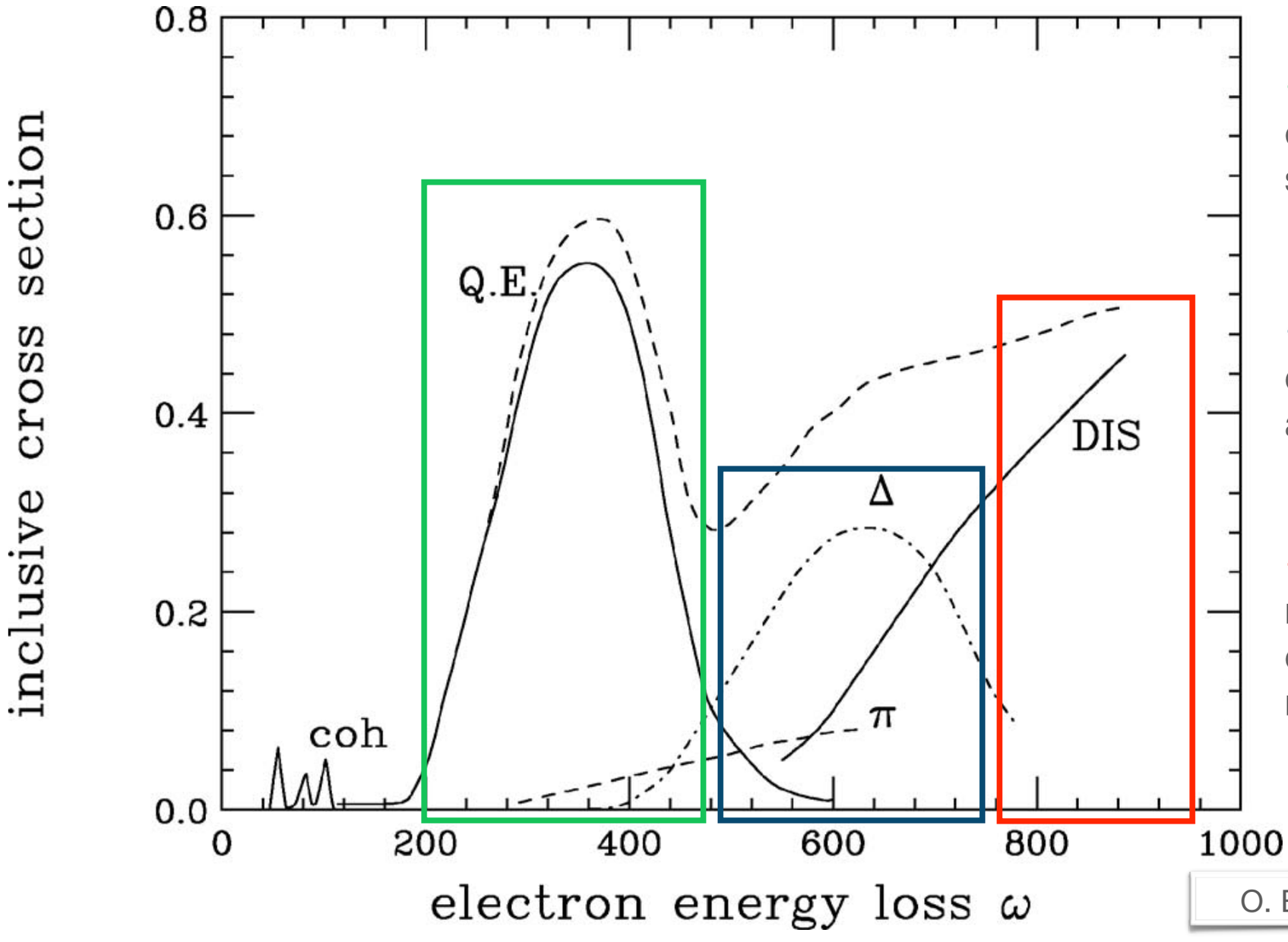


- Broad peak due to quasi-elastic electron-nucleon scattering.
- Excitation of the nucleon to distinct resonances (like the Δ) and pion production.
- Deep Inelastic Scattering region, productions of hadrons other than protons and neutrons

O. Benhar, et al. RMP **80**, 189 (2008)

The different reaction mechanisms can be easily identified

# Neutrinos' challenge

*"Neutrinos ... win the minimalist contest: zero charge, zero radius, and very possibly zero mass."*

—Leon M. Lederman—

- In neutrino-oscillation experiments the use of nuclear target as detectors allows for a substantial increase of the event rate.

- Understanding neutrino-nucleus interactions in the 1-10 GeV spectrum requires an accurate description of both nuclear dynamics and of the interaction vertex where relativistic effects are accounted for

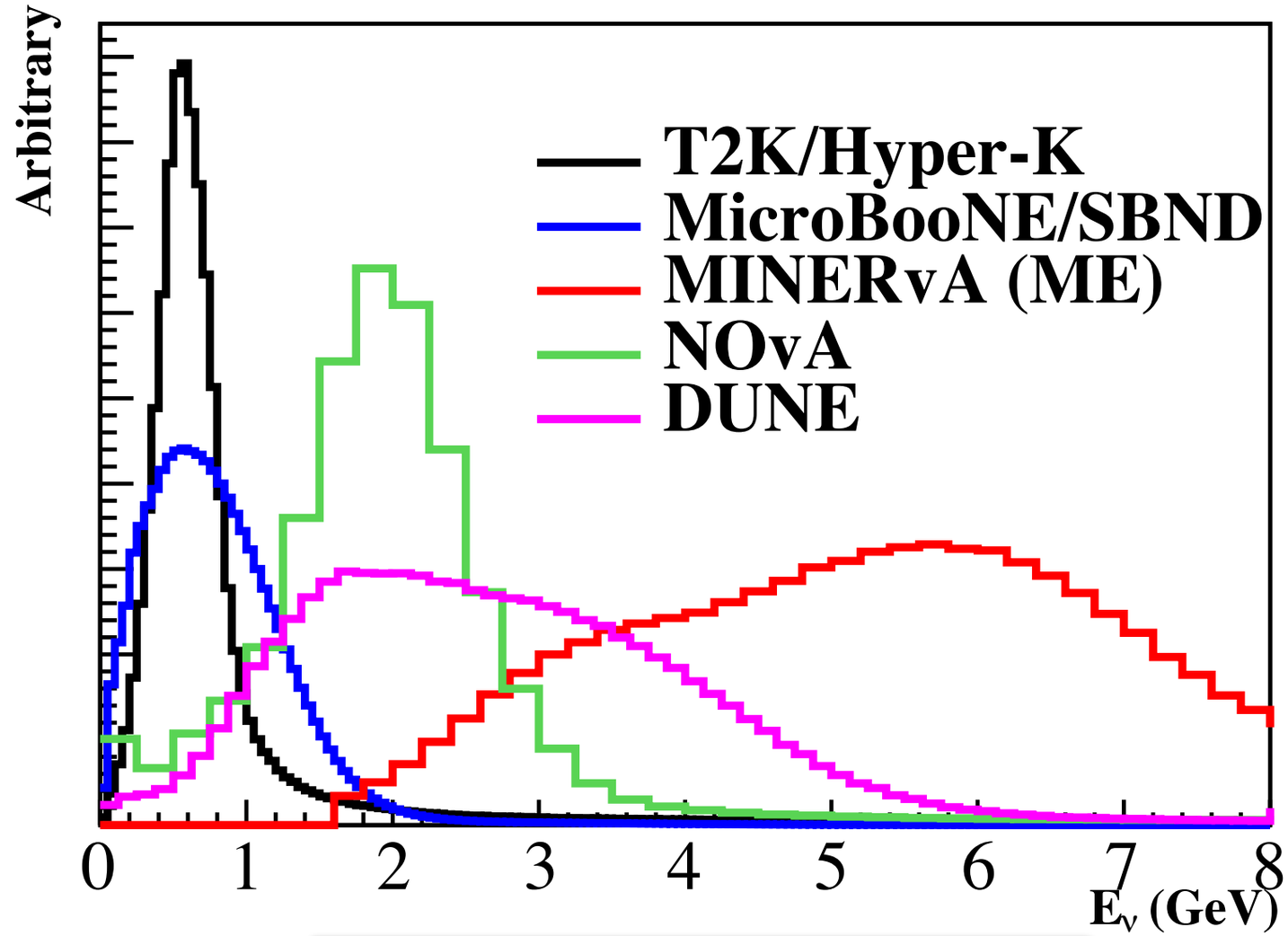


T. Katori and M. Martini,. arXiv:1611.07770

# Outline

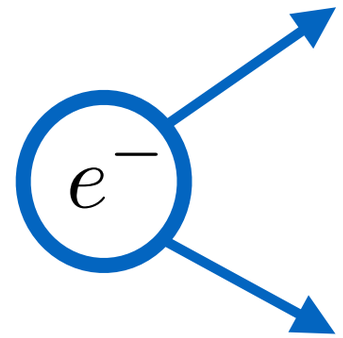


Green's Function Monte Carlo

Self Consistent Green's Function SF
+ Impulse Approximation

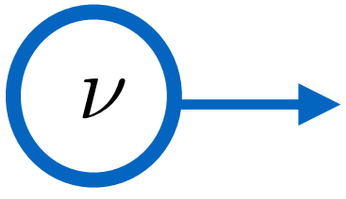


Correlated Basis Function SF
+ Impulse Approximation

# Electron-nucleus scattering

The inclusive cross section of the process in which a lepton scatters off a nucleus and the hadronic final state is undetected can be written as

$$\frac{d^2\sigma}{d\Omega_\ell dE_{\ell'}} = L_{\mu\nu}W^{\mu\nu}$$

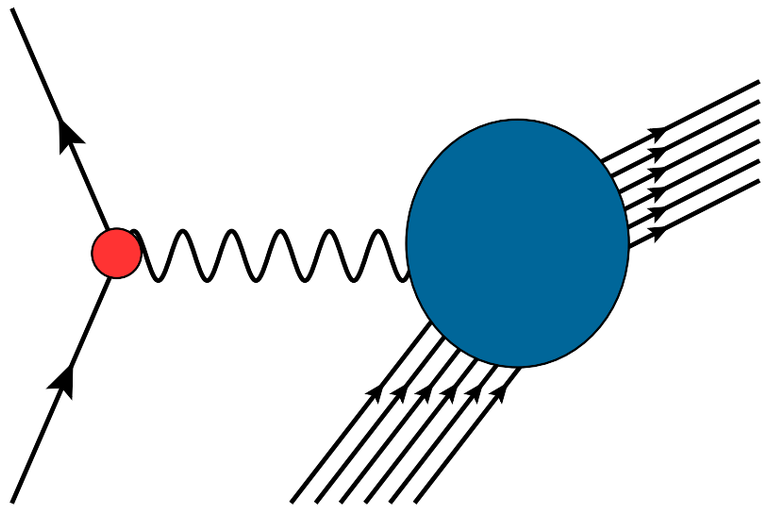

- The Leptonic tensor is fully specified by the lepton kinematic variables. For instance, in the electron-nucleus scattering case

$$L^{\mathrm{EM}}_{\mu\nu} = 2[k_\mu k'_\nu + k_\nu k'_\mu - g_{\mu\nu}(kk')]$$

- The Hadronic tensor contains all the information on target response

$$W^{\mu\nu} = \sum_f \langle 0|J^{\mu\,\dagger}(q)|f\rangle\langle f|J^\nu(q)|0\rangle\delta^{(4)}(p_0 + q - p_f)$$

Non relativistic nuclear many-body theory (NMBT) provides a fully consistent theoretical approach allowing for an accurate description of |0>, independent of momentum transfer.

# Non relativistic Nuclear Many Body Theory

• Within NMBT the nucleus is described as a collection of A point-like nucleons, the dynamics of which are described by the non relativistic Hamiltonian

$$H = \sum_i \frac{\mathbf{p}_i^2}{2m} + \sum_{i<j} v_{ij} + \sum_{i<j<k} V_{ijk} + \dots$$

The nuclear energy spectrum can be accurately determined

$$H\,|0\rangle = E_0\,|0\rangle \quad , \quad H\,|f\rangle = E_f\,|f\rangle$$

The nuclear electromagnetic current is constrained through the continuity equation

$$\boldsymbol{\nabla} \cdot \mathbf{J}_{\rm EM} + i[H, J^0_{\rm EM}] = 0$$

• The above equation implies that $\mathbf{J}_{\rm EM}$ involves two-nucleon contributions.

• Non relativistic expansion of $\mathbf{J}_{\rm EM}$, powers $|\mathbf{q}|/m$

# The Green's Function Monte Carlo approach

- Green's function Monte Carlo combined with a realistic nuclear hamiltonian reproduces the spectra of light nuclei

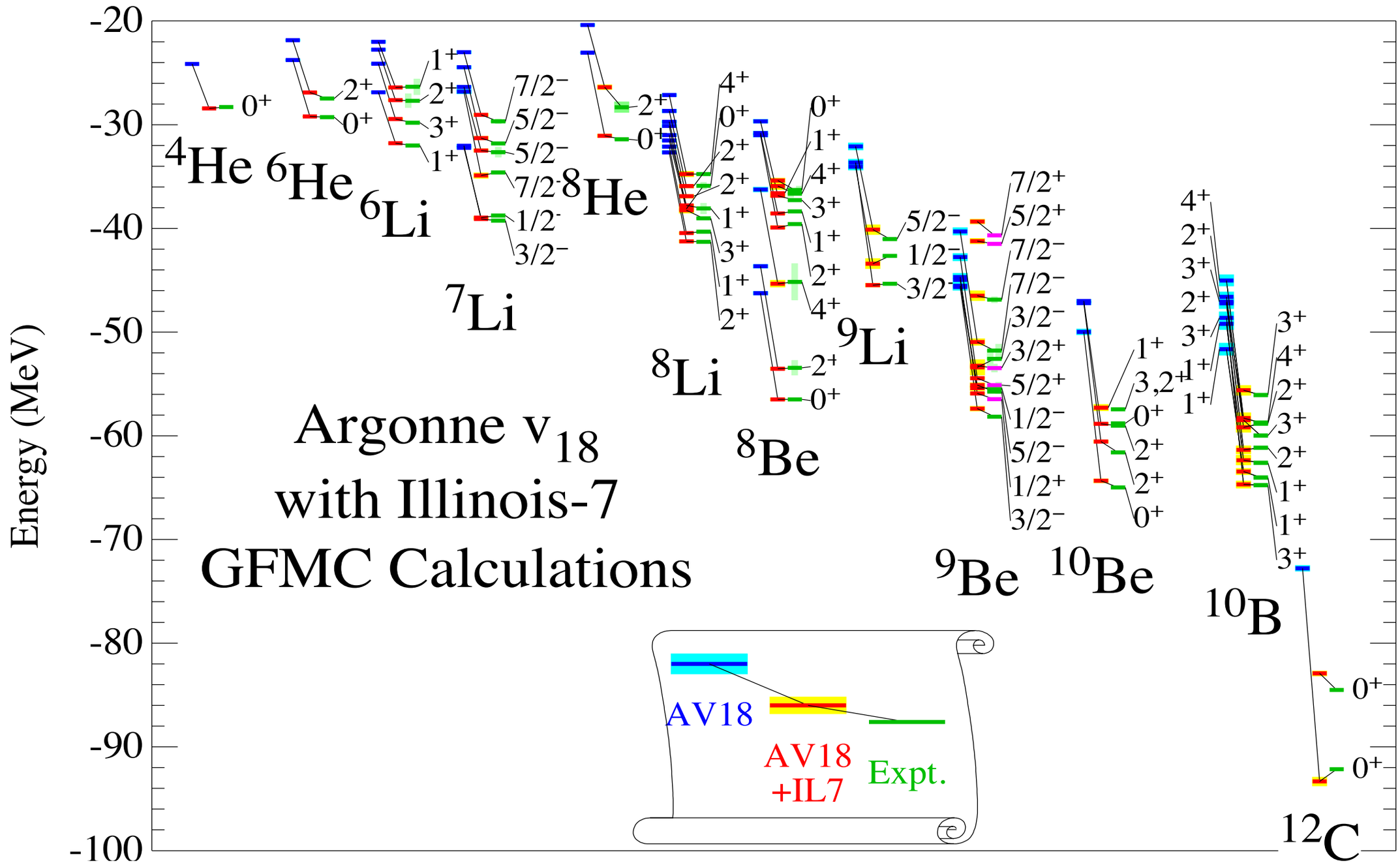

# The Green's Function Monte Carlo approach

✤ Accurate GFMC calculations of the electromagnetic responses of $^4$He and $^{12}$C have been recently performed: A. Lovato et al, Phys.Rev.Lett. 117 (2016), 082501, Phys.Rev. C97 (2018), 022502

$$R_{\alpha\beta}(\omega, \mathbf{q}) = \sum_f \langle 0|J^\dagger_\alpha(\mathbf{q})|f\rangle\langle f|J_\beta(\mathbf{q})|0\rangle\delta(\omega - E_f + E_0)$$

• Valuable information on the energy dependence of the response functions can be inferred from the their Laplace transforms

$$E_{\alpha\beta}(\mathbf{q}, \tau) = \int d\omega\, e^{-\omega\tau} R_{\alpha\beta}(\mathbf{q}, \omega) = \langle 0|J^\dagger_\alpha(\mathbf{q}) e^{-(H-E_0)\tau} J_\beta(\mathbf{q})|0\rangle$$

Using the completeness relation for the final states, we are left with ground-state expectations value

## Limitations of the original method:

★ It is a nonrelativistic method, can not be safely applied in the entire kinematical region relevant for neutrino experiments ⟶ two fragment model, see Alessandro's talk on Monday

★ The computational effort required by the inversion of $E_{\alpha\beta}$ makes the direct calculation of inclusive cross sections unfeasible ⟶ novel algorithm based on first-kind scaling

# Scaling in the Fermi gas model

• Scaling of the first kind: the nuclear electromagnetic responses divided by an appropriate function describing single-nucleon physics no longer depend on the two variables $\omega$ and $\mathbf{q}$, but only upon $\psi(\mathbf{q},\omega)$

Adimensional variables:

$$\lambda = \omega/2m$$
$$\kappa = |\mathbf{q}|/2m$$
$$\tau = \kappa^2 - \lambda^2$$

$$\eta_F = p_F/m$$
$$\xi_F = \sqrt{p_F^2 + m^2}/m - 1$$

Scaling function:

$$\psi = \frac{1}{\xi_F} \frac{\lambda - \tau}{\sqrt{(1+\lambda)\tau + \kappa\sqrt{\tau(1+\tau)}}}$$

In the FG the L and T responses have the same functional form :

$$R_{L,T} = (1-\psi^2)\theta(1-\psi^2) \times G_{L,T}$$

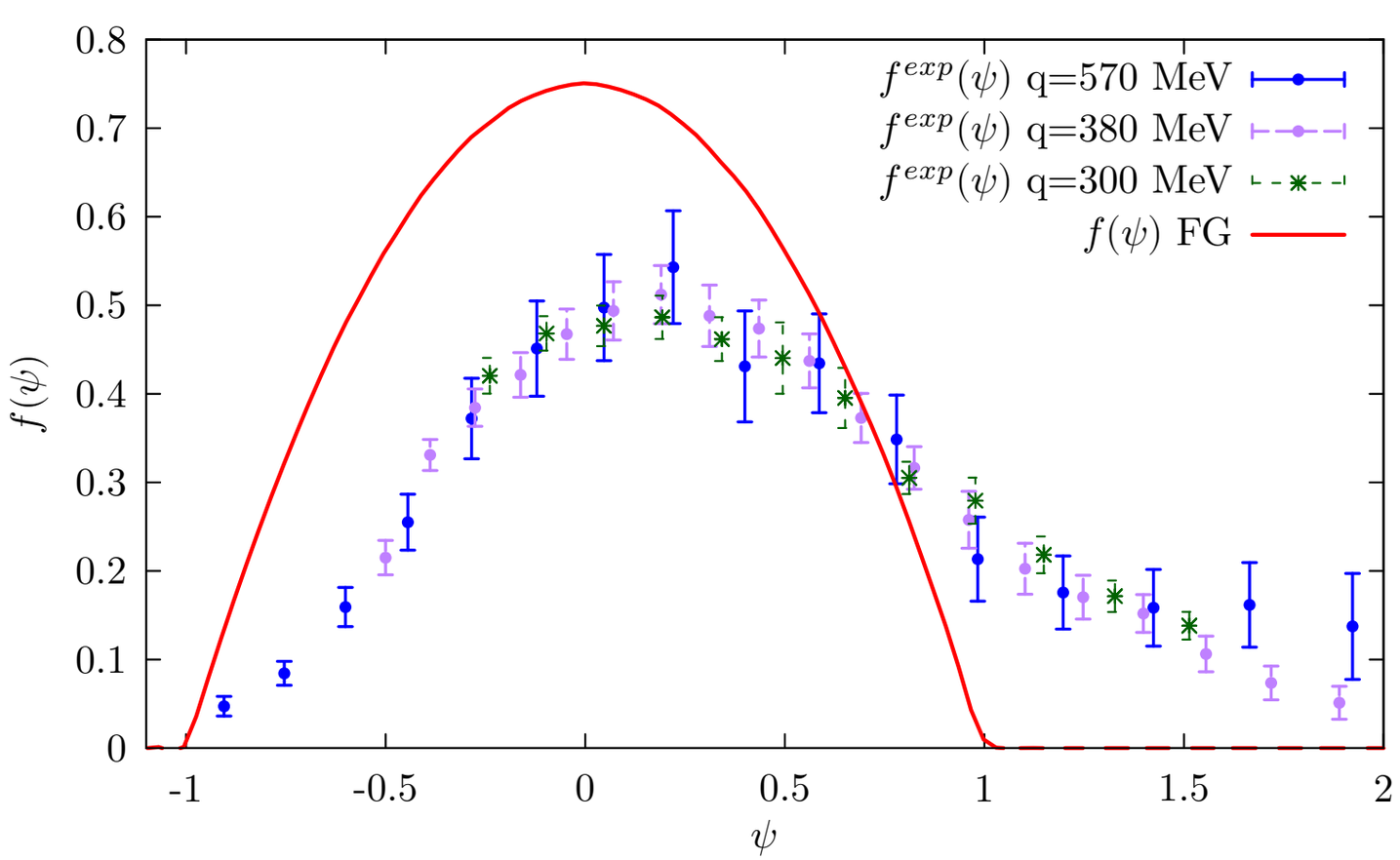

# Scaling as an interpolation tool

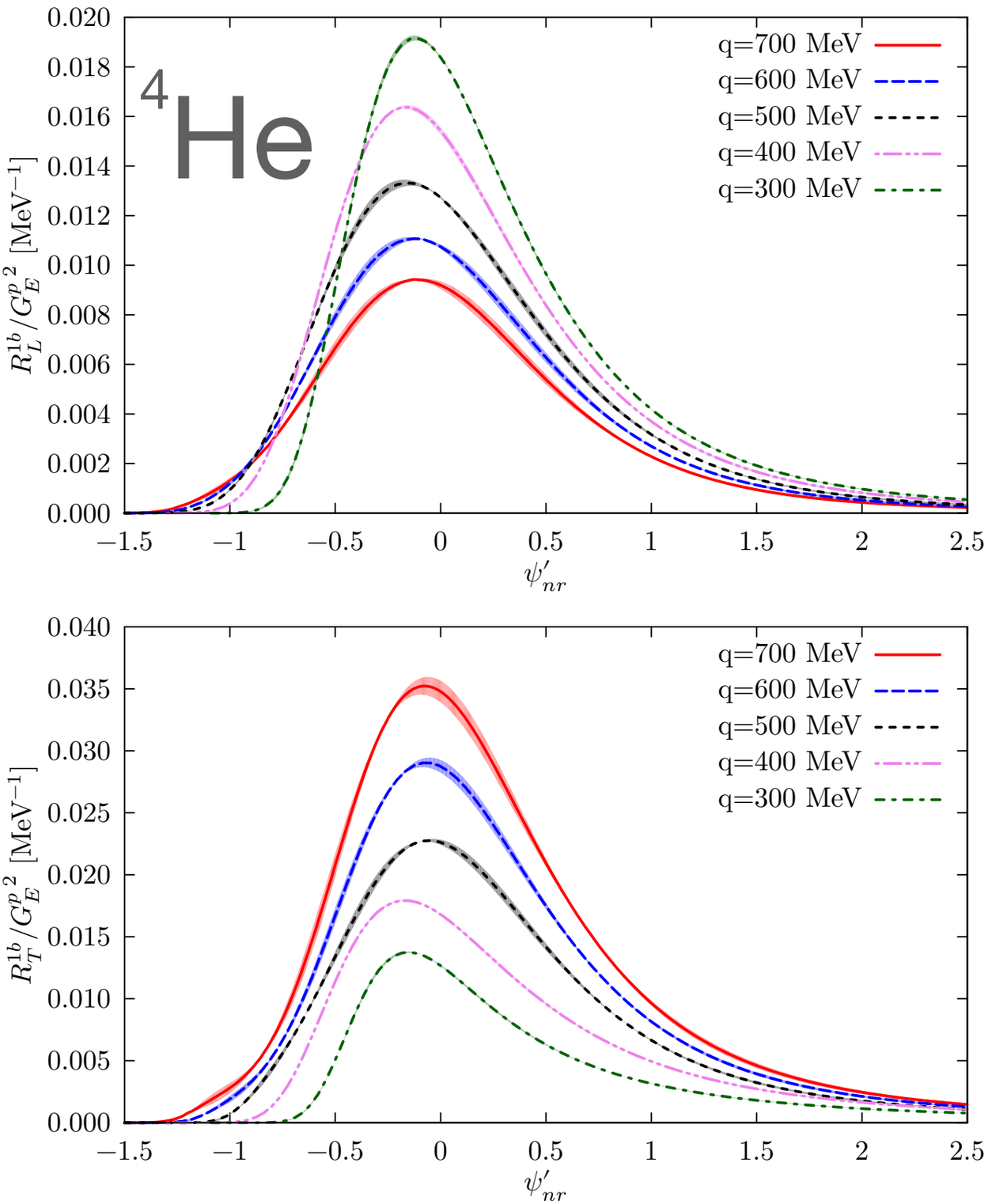


- To compute inclusive electron-nucleus cross sections we developed a novel interpolation algorithm based on the scaling of the nuclear responses.

- For a fixed value of $E_e$ and $\theta_e$

$$Q^2 = 4E_e(E_e - \omega)\sin^2\frac{\theta_e}{2}\ , |\mathbf{q}| = \sqrt{Q^2 + \omega^2}$$

- We first compute $\psi'_{nr}$ then the set of $R_{L,T}(\psi'_{nr}, \mathbf{q})$ is interpolated in $|\mathbf{q}|$.

- For a given value of $\psi'_{nr}$ the curves corresponding to different values of $|\mathbf{q}|$ are almost perfectly aligned and monotonic functions of $|\mathbf{q}|$. Using the concept of scaling, largely improves the accuracy of the interpolation procedure and reduces the computational cost

# Scaling as a tool to interpolate the responses

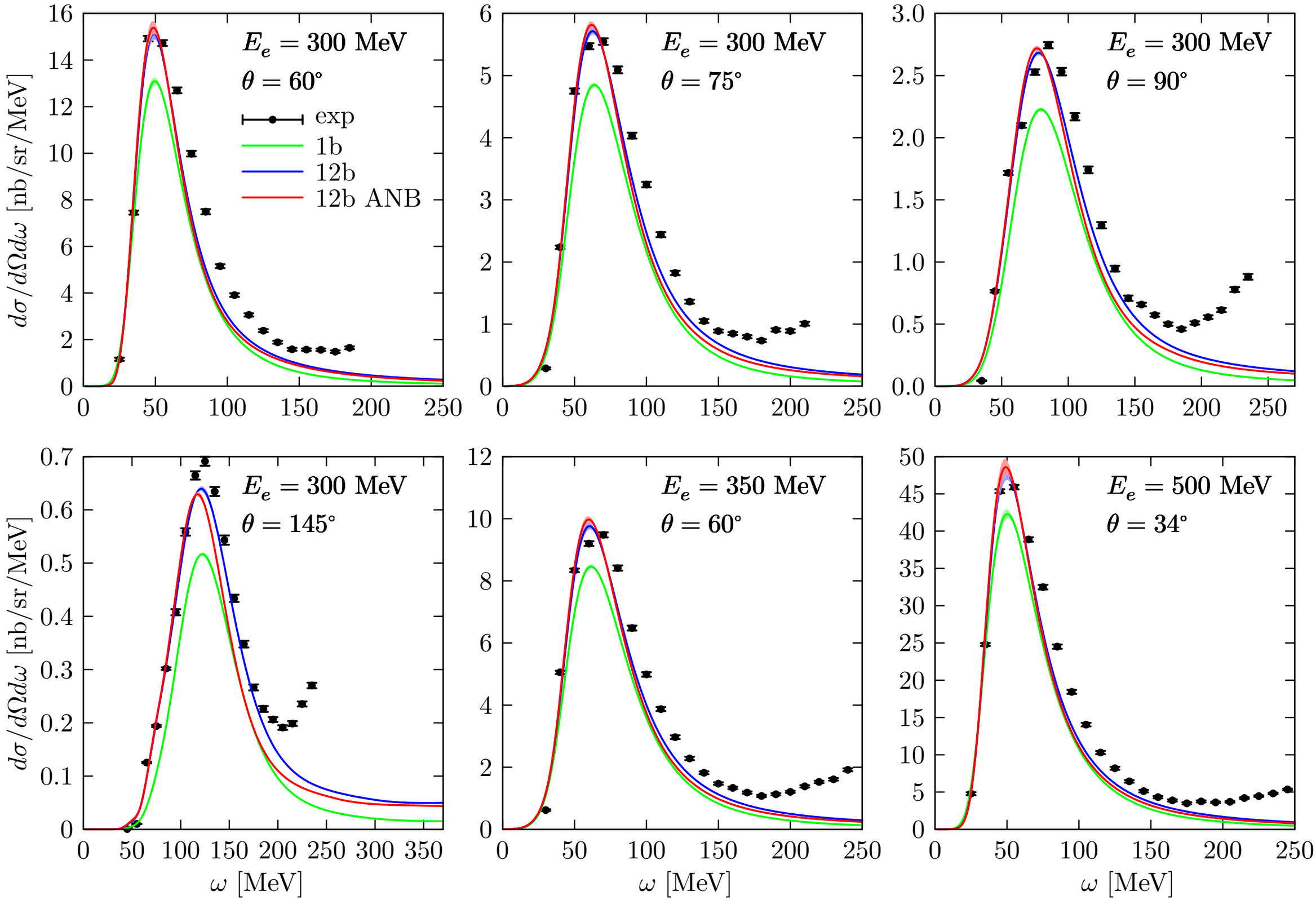

# Scaling as a tool to interpolate the responses

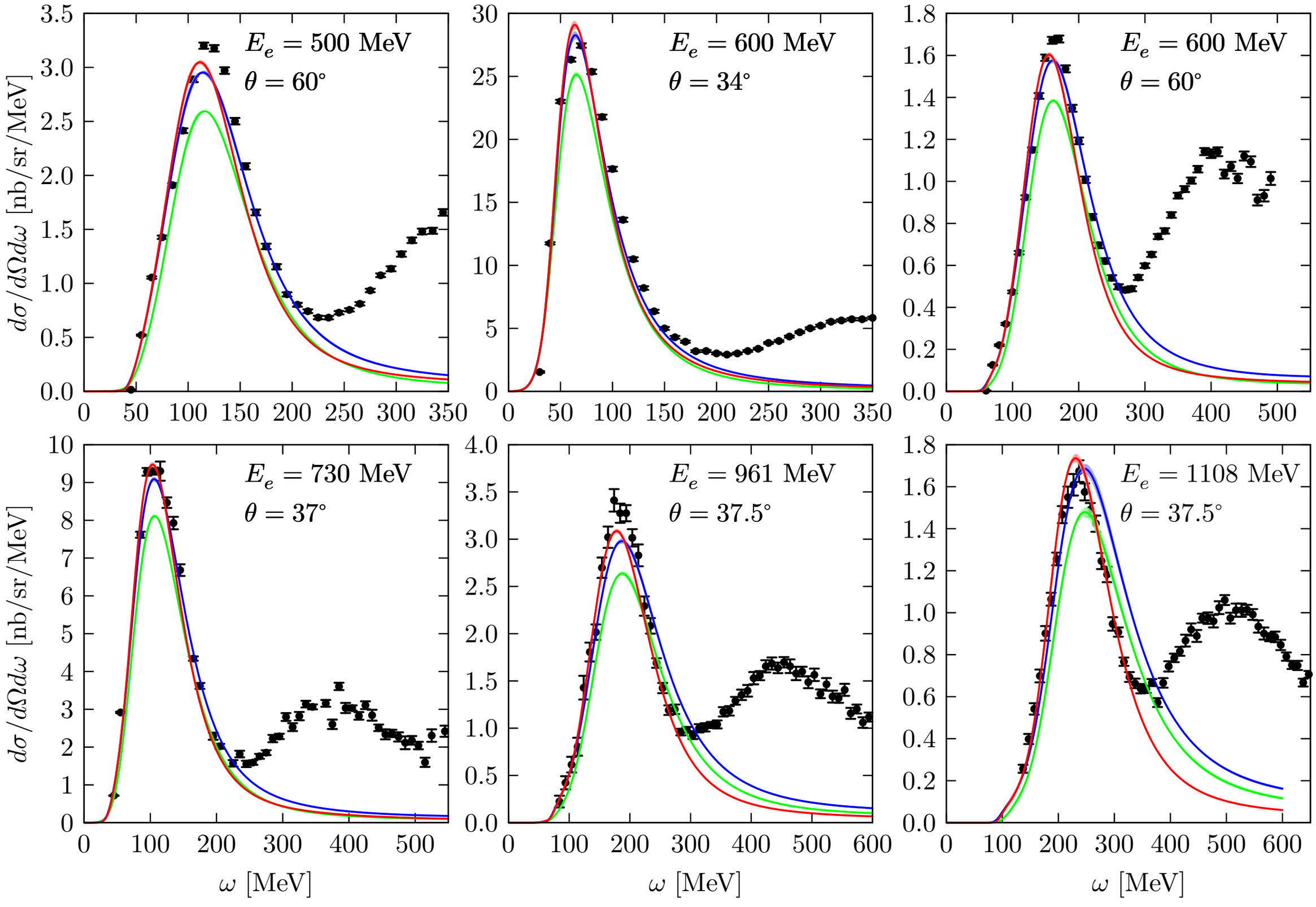

# Self Consistent Green's Function

- The one-body Green's function is completely determined by solving the Dyson equation

$$G_{\alpha\beta}(E) = G^0_{\alpha\beta}(E) + \sum_{\gamma\delta} G^0_{\alpha\gamma}\Sigma^*_{\gamma\delta}(E)G_{\delta\beta}(E)$$

$G^0_{\alpha\beta}(E)$: initial reference state, HF

$\Sigma^*_{\gamma\delta}(E)$: Self energy: encoding nuclear medium effects on the particle propagation

$G_{\delta\beta}(E)$: Correlated propagator

- $\Sigma^* = \Sigma^*[G(E)]$, an iterative procedure is required to solve the Dyson equation self-consistently

- The self-energy is systematically calculated in a non-perturbative fashion within the Algebraic Diagrammatic Construction (ADC).

- Two- and three-nucleon force contributions are included up to the third order → ADC(3)

- Chiral $NNLO_{sat}$ two and three nucleon forces are used in the calculation

# Self Consistent Green's Function

- To reduce the number of Feynman diagrams entering the calculation of the Green's Function, only interaction irreducible diagrams are considered. The effective one- and two- body interactions are introduced:

$$\tilde{U}_{\alpha\beta} = U_{\alpha\beta} + \sum_{\delta\gamma} V_{\alpha\gamma,\beta\delta}\rho_{\delta\gamma} + \frac{1}{4}\sum_{\mu\nu\gamma\delta} W_{\alpha\mu\nu,\beta\gamma\delta}\rho_{\gamma\mu}\rho_{\nu\delta} \ ,$$

$$\tilde{V}_{\alpha\beta,\delta\gamma} = V_{\alpha\beta,\delta\gamma} + \sum_{\mu\nu} W_{\alpha\beta\mu,\gamma\delta\nu}\rho_{\nu\mu} \ .$$

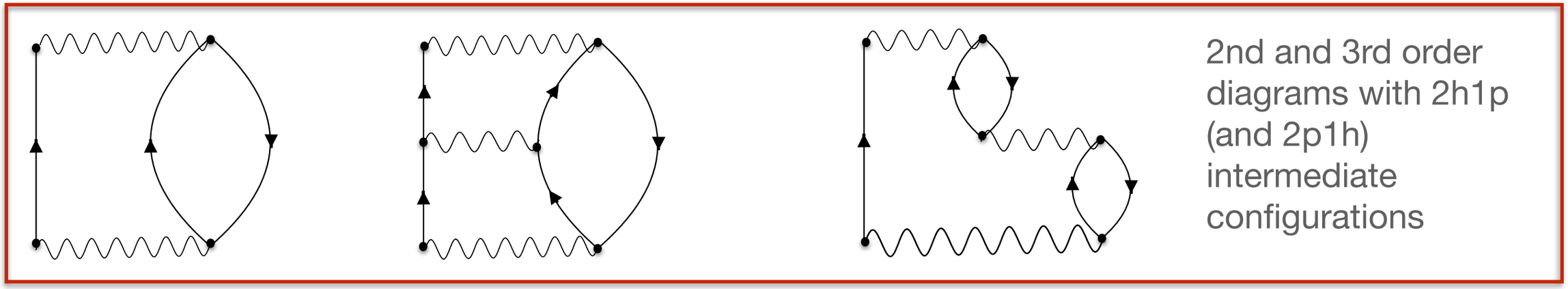


- Within the ADC(3) these diagrams are taken as 'seeds' for the infinite order re-summation that eventually generates the self-energy

- Use the one-body propagator to obtain static and dynamical nuclear observables of $^{4}$He and $^{16}$O.

# The $^4$He SGFC point density distribution

• Operators are expanded on an harmonic oscillator basis with a given oscillator frequency $\hbar\omega$ , and size of the single-particle model space $N_{max}$

• Point-proton density distribution

$$\rho_p(\mathbf{r}) = \sum_{\alpha\beta} \phi^*_\beta(\mathbf{r})\phi_\alpha(\mathbf{r})\rho_{\alpha\beta}$$

• One-body density matrix

$$\rho_{\alpha\beta} = \langle \Psi^A_0 | a^\dagger_\beta a_\alpha | \Psi^A_0 \rangle$$

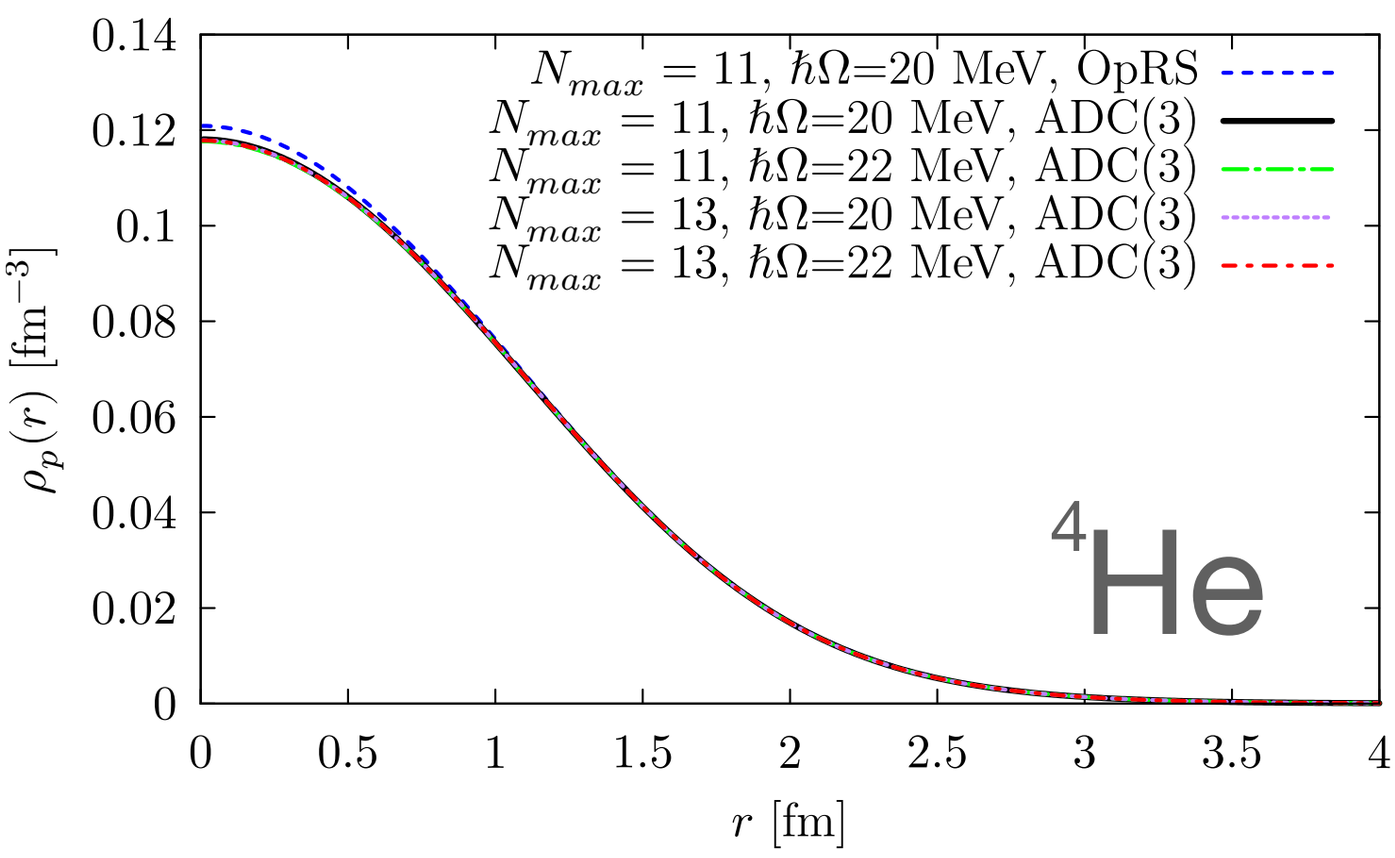


• The Optimized Reference State (OpRS) curve is obtained defining an independent particle model propagator:

$$G^{\mathrm{OpRS}}_{\alpha\beta}(E) = +\sum_{k\in F} \frac{\phi^k_\alpha(\phi^k_\beta)^*}{E - \epsilon^{\mathrm{OpRS}}_k - i\eta}$$

• $\epsilon^{\mathrm{OpRS}}$ and $\phi$ are obtained by requiring that the OpRS lowest momenta of the spectral distribution reproduce those of the full calculation

# The $^4$He SGFC charge density distribution

- The nuclear charge density distribution is written in terms of the charge elastic form factor

$$\rho_{ch}(r') = \int \frac{d^3q}{(2\pi)^3} e^{-i\mathbf{q}\cdot\mathbf{r}'} \frac{(G_E^p(Q_{el}^2 + G_E^n(Q_{el}^2))\tilde{\rho}_p(q)}{\sqrt{1+Q_{el}^2/(4m^2)}}$$

- The cOm issue: The subtraction of the cOm contribution from the wave function is a long standing problem affecting a number of many-body approaches relying on single-nucleon basis

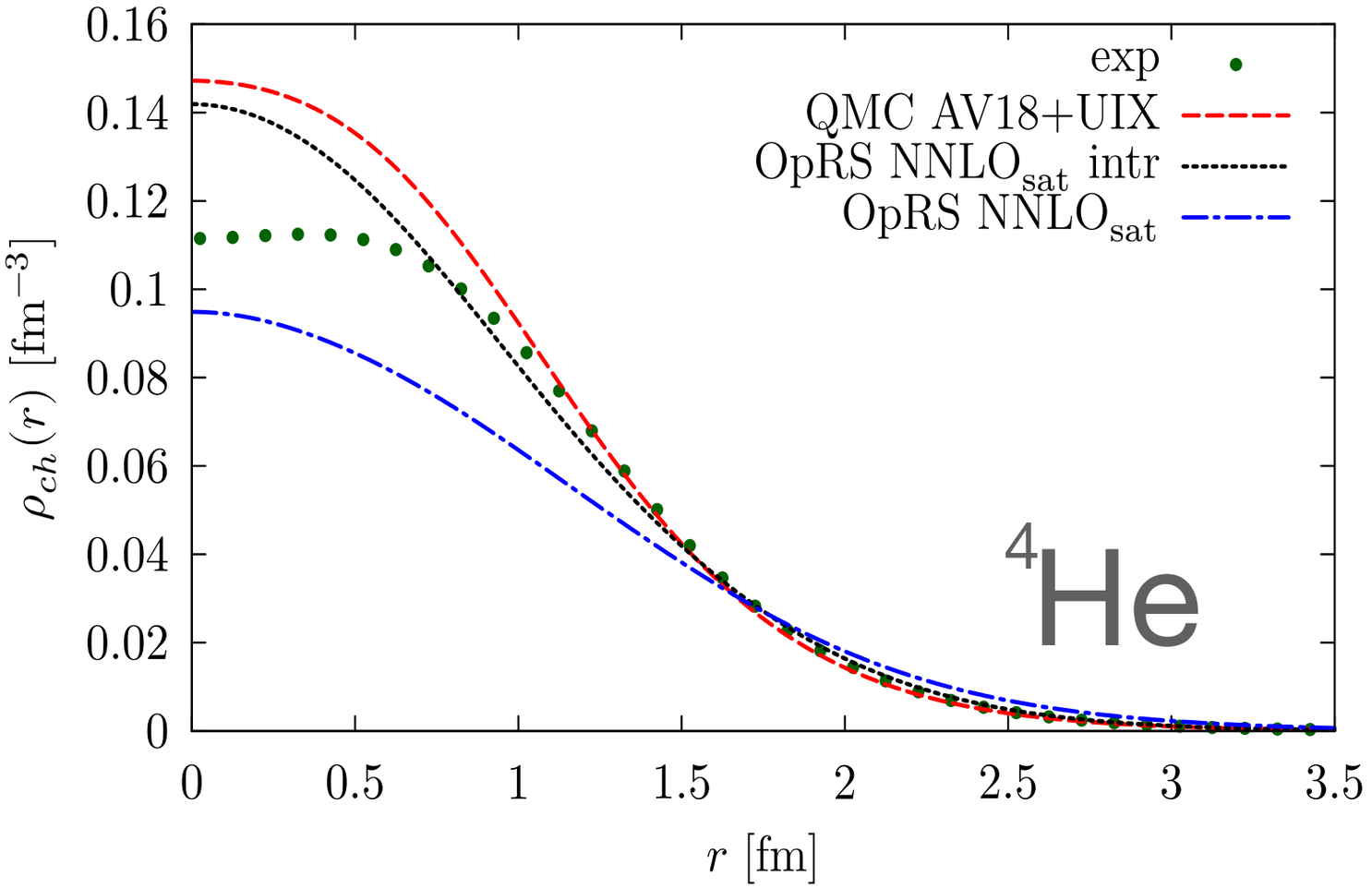


To estimate the error due to residual cOm contribution in $^4$He we developed Metropolis Monte Carlo calculation

- Trial wave function: $|\psi_V\rangle = |\psi_0^{OpRS}\rangle$

- A sequence of points in the 3A-dimensional space are generated by sampling from $P(\mathbf{R}) = |\psi_0^{OpRS}(\mathbf{R})|^2$

- The intrinsic coordinates are given by

$$\tilde{\mathbf{r}}_i = \mathbf{r}_i - \mathbf{R}_{cm} \ , \ \mathbf{R}_{cm} = \frac{1}{A}\sum_i \mathbf{r}_i$$

✤ The QMC AV18+UIX results are taken from D. Lonardoni et al, Phys. Rev. C96, 024326 (2017)

# The charge elastic form factor $^4$He

- The charge elastic form factor is given by $F_L(\mathbf{q}) = \frac{1}{Z} \frac{G_E^p(Q_{el}^2)\tilde{\rho}_p(q) + G_E^n(Q_{el}^2)\tilde{\rho}_n(q)}{\sqrt{1 + Q_{el}^2/(4m^2)}}$ ,

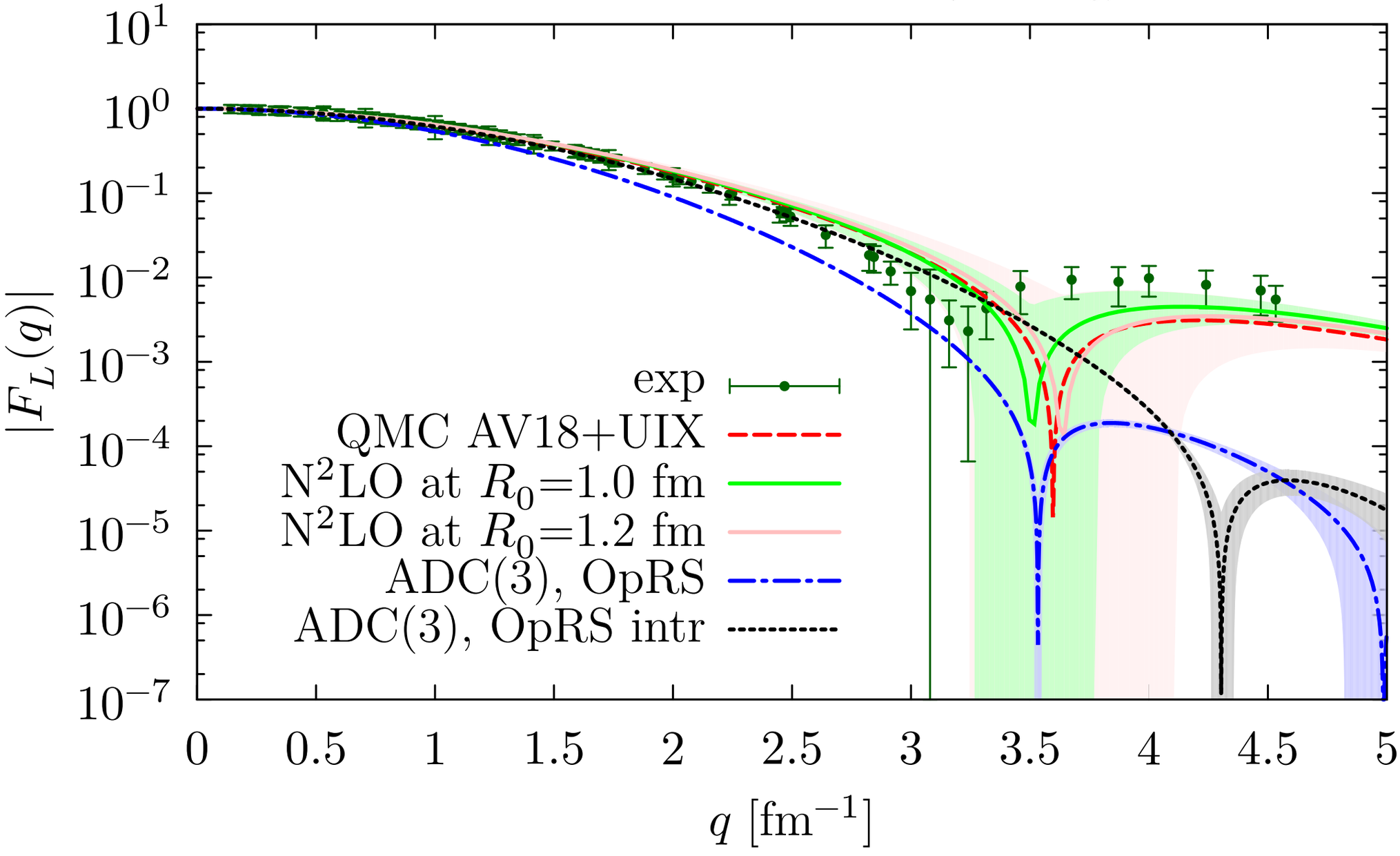


✤ The N$^2$LO results are taken from J. E. Lynn et al, Phys. Rev. C 96, 054007 (2017) where two different coordinate space cut offs have been adopted

# The $^{16}$O SGFC charge density distribution

- Nuclear charge density distribution of $^{16}$O

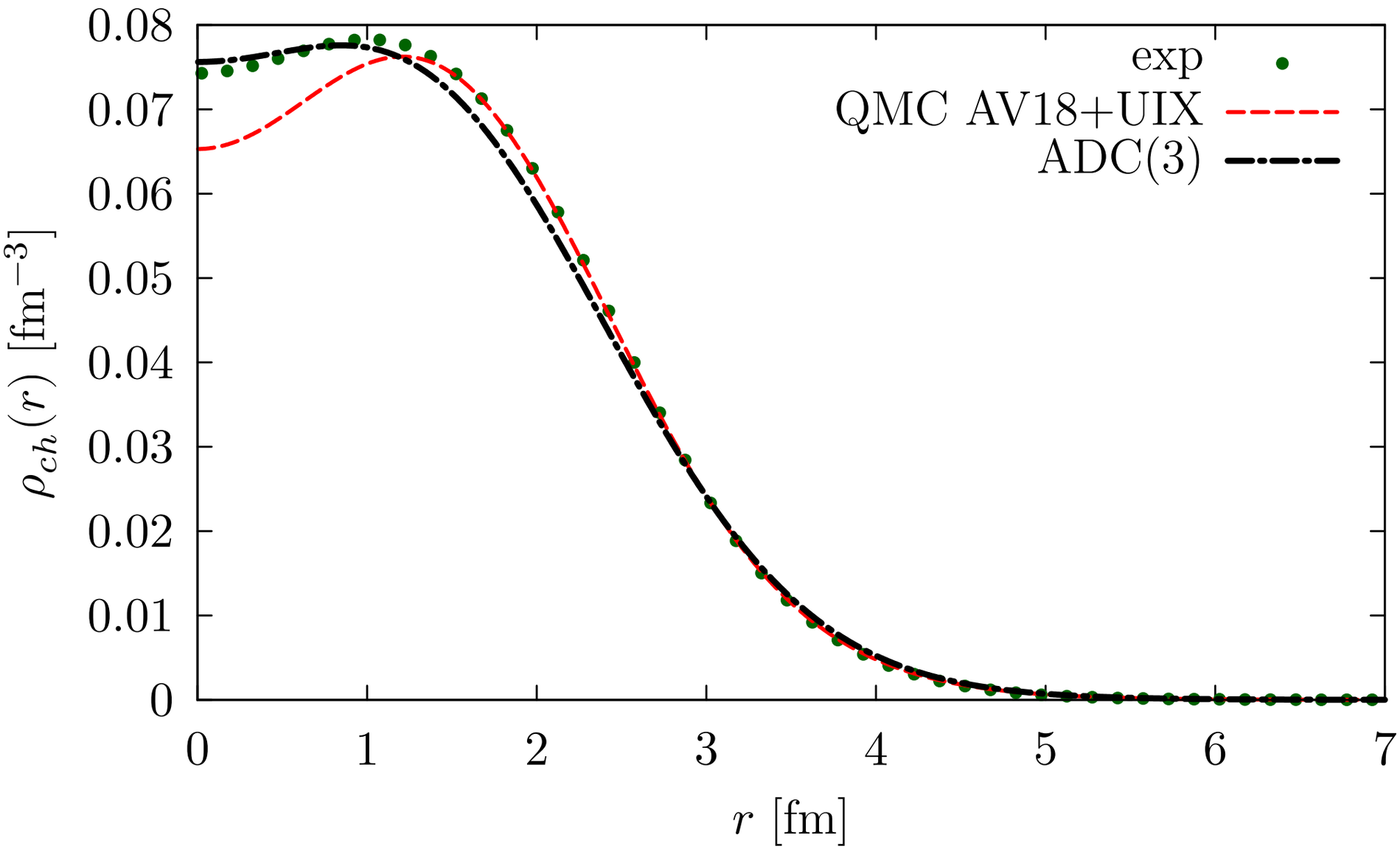


- Nice agreement between the SCGF and QMC calculations

- SCGF results agree with experiments (corroborates the goodness of NNLO$_{sat}$)

# The $^{16}$O SGFC momentum distribution

- Single particle momentum distribution of $^{16}$O

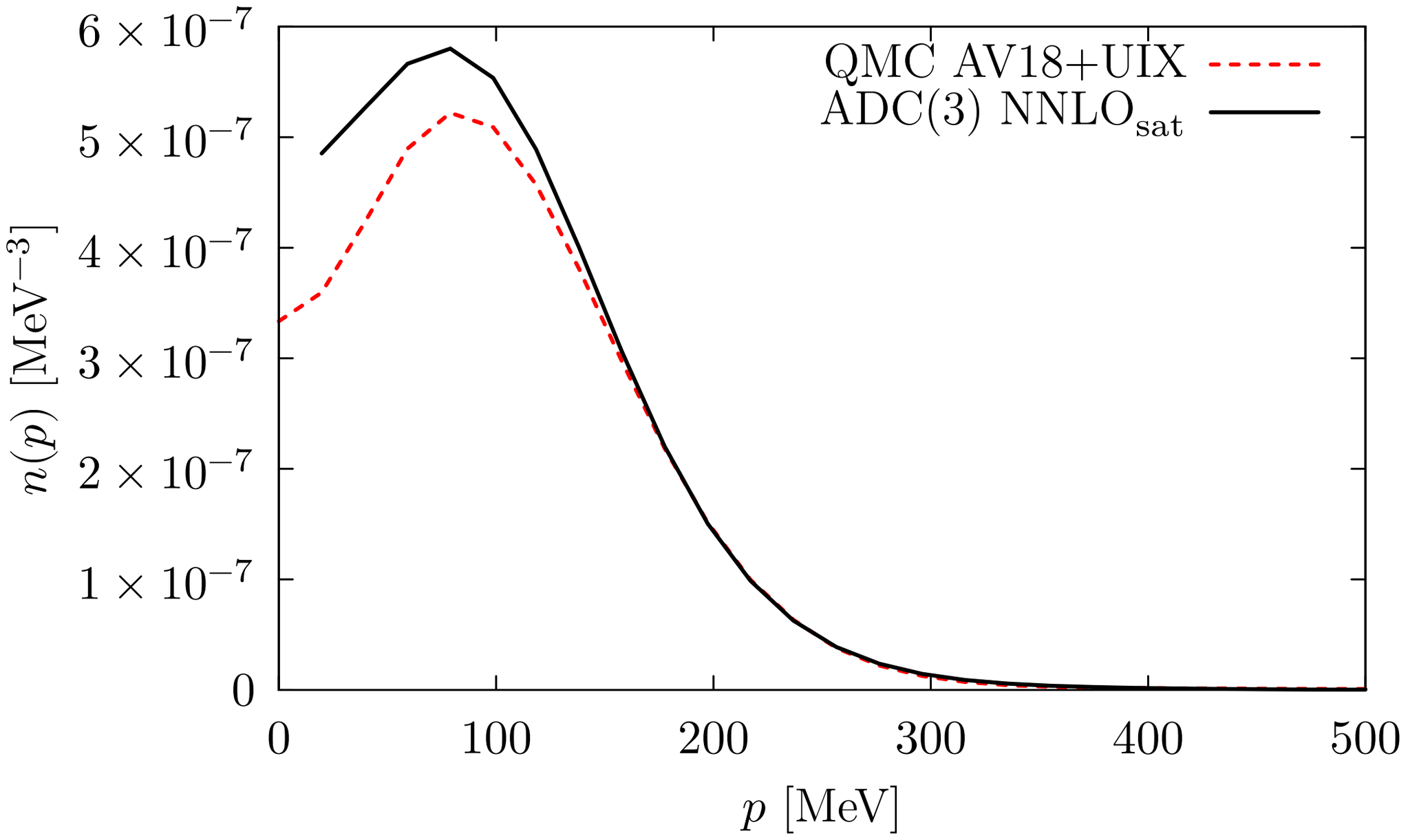


- The momentum distribution reflects the fact that NNLO$_{\mathrm{sat}}$ is softer the AV18+UIX.

# The $^{16}$O SGFC momentum distribution

- Single particle momentum distribution of $^{16}$O, log scale

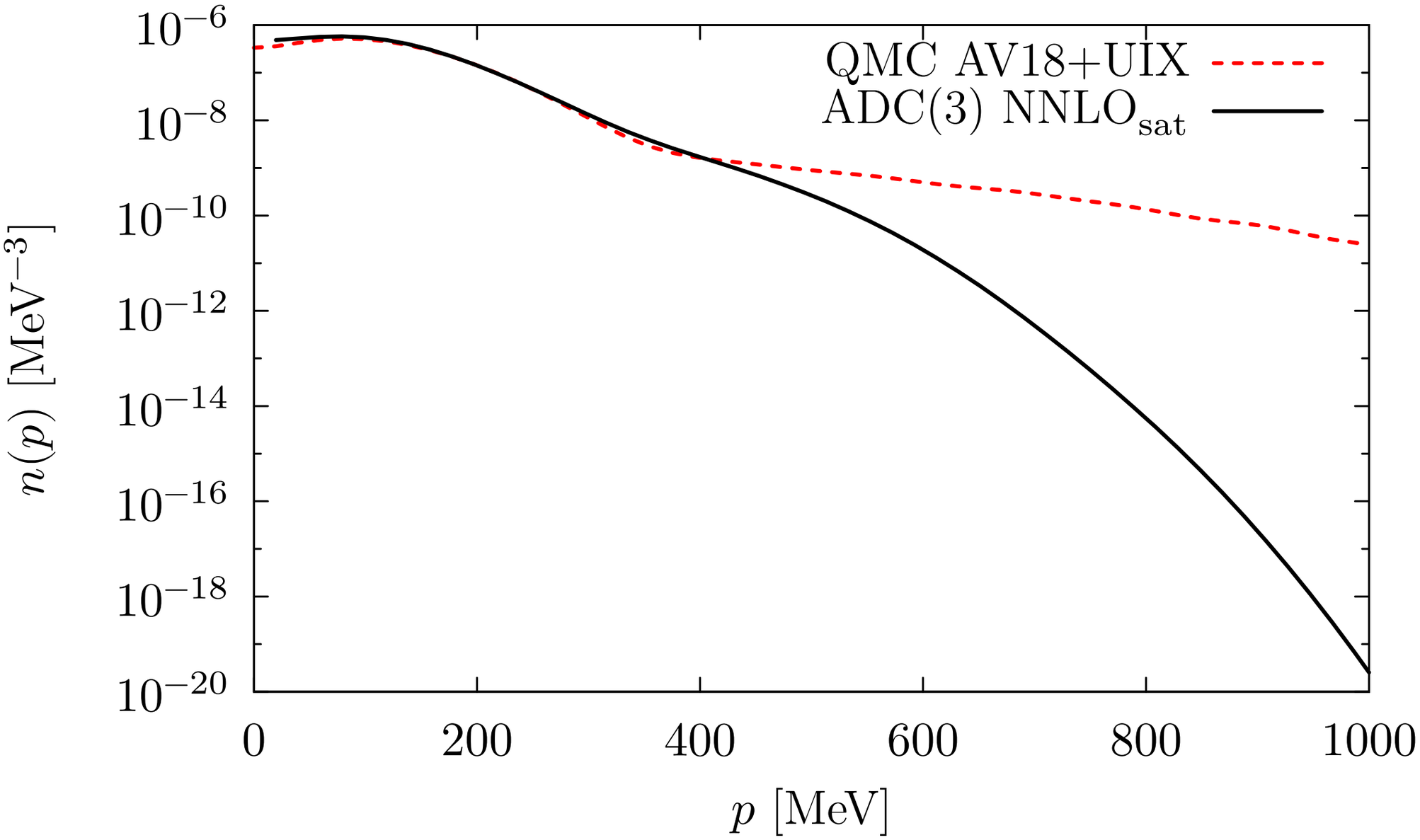


- The momentum distribution reflects the fact that NNLO$_{\rm sat}$ is softer the AV18+UIX.

# The charge elastic form factor for $^{16}$O

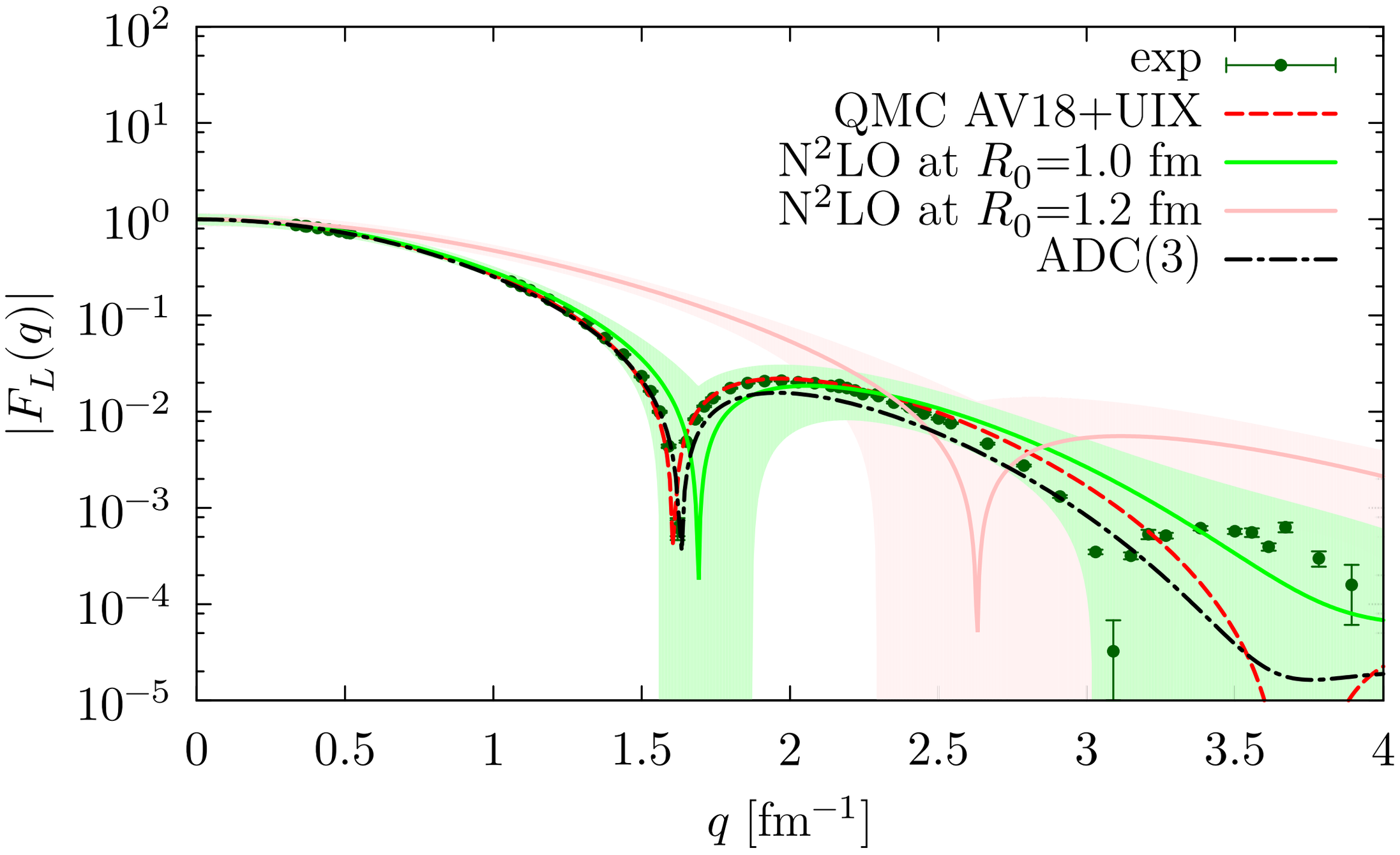


✤ The N$^2$LO results are taken from D. Lonardoni, et. al, Phys. Rev. C97, 044318 (2018) where two different coordinate-space cutoffs have been adopted

# The Impulse Approximation

- For sufficiently large values of |**q**|, the IA can be applied under the assumptions

$$|f\rangle \longrightarrow |p\rangle \otimes |f\rangle_{A-1}$$

$$J_\alpha = \sum_i j_\alpha^i$$

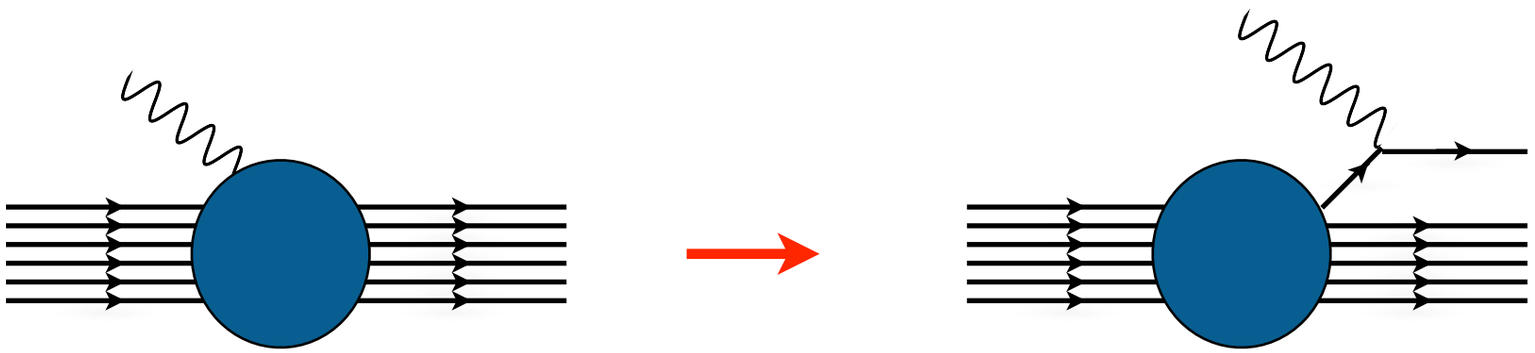

- The matrix element of the current can be written in the factorized form

$$\langle 0|J_\alpha|f\rangle \rightarrow \sum_k \langle 0|[|k\rangle \otimes |f\rangle_{A-1}]\langle k| \sum_i j_\alpha^i |p\rangle$$

- The nuclear cross section is given in terms of the one describing the interaction with individual bound nucleons

$$d\sigma_A = \int dE\, d^3k d\sigma_N P(\mathbf{k}, E)$$

- The intrinsic properties of the nucleus are described by the hole spectral function

# The one-body hole Spectral Function

- The nuclear matrix element can be rewritten in terms of the transition amplitude

$$[\langle\psi_f^{A-1}|\otimes\langle k|]|\psi_0^A\rangle = \sum_\alpha \mathcal{Y}_{f,\alpha}\tilde{\Phi}_\alpha(\mathbf{k}) = \sum_\alpha \tilde{\Phi}_\alpha(\mathbf{k})\langle\psi_f^{A-1}|a_\alpha|\psi_0^A\rangle\,,$$

- The Spectral Function gives the probability distribution of removing a nucleon with momentum **k**, leaving the spectator system with an excitation energy E

$$P_h(\mathbf{k},E) = \sum_f |\langle\psi_0^A|[|\mathbf{k}\rangle\otimes|\psi_f^{A-1}\rangle]|^2\delta(E+E_f^{A-1}-E_0^A)$$
$$= \frac{1}{\pi}\sum_{\alpha\beta}\tilde{\Phi}^*_\beta(\mathbf{k})\tilde{\Phi}_\alpha(\mathbf{k})\mathrm{Im}\langle\psi_0^A|a^\dagger_\beta\frac{1}{E+(H-E_0^A)-i\epsilon}a_\alpha|\psi_0^A\rangle\,.$$

- The two points Green's Function describes nucleon propagation in the nuclear medium

$$G_{h,\alpha\beta}(E) = \langle\psi_0^A|a^\dagger_\beta\frac{1}{E+(H-E_0^A)-i\epsilon}a_\alpha|\psi_0^A\rangle$$

# The Impulse Approximation and convolution scheme

• In the kinematical region in which the interactions between the struck particle and the spectator system can not be neglected, the IA results have to be modified to include the effect of final state interactions (FSI).

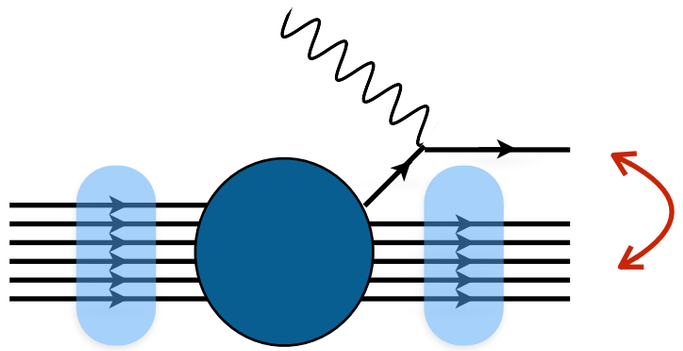

$$d\sigma_{FSI} = \int d\omega' f_{\mathbf{q}}(\omega - \omega') d\tilde{\sigma}_{IA} \quad , \quad \tilde{e}(\mathbf{p}) = e(\mathbf{p}) + \mathcal{U}(t_{kin}(\mathbf{p}))$$

Optical Potential

• The theoretical approach to calculate the folding function consists on a generalization of Glauber theory of high energy proton-nucleus scattering

$$f_{\mathbf{q}}(\omega) = \delta(\omega)\sqrt{T_{\mathbf{q}}} + \int \frac{dt}{2\pi} e^{i\omega t} \left[ \bar{U}_{\mathbf{q}}^{FSI}(t) - \sqrt{T_{\mathbf{q}}} \right]$$

Nuclear Transparency

Glauber Factor

A.Ankowski et al,Phys. Rev. D91, 033005 (2015)

O.Benhar, Phys. Rev. C87, 024606 (2013)

# $^4$He-e$^-$ cross sections within the SCGF approach

- ADC(3) and OpRS results: IA

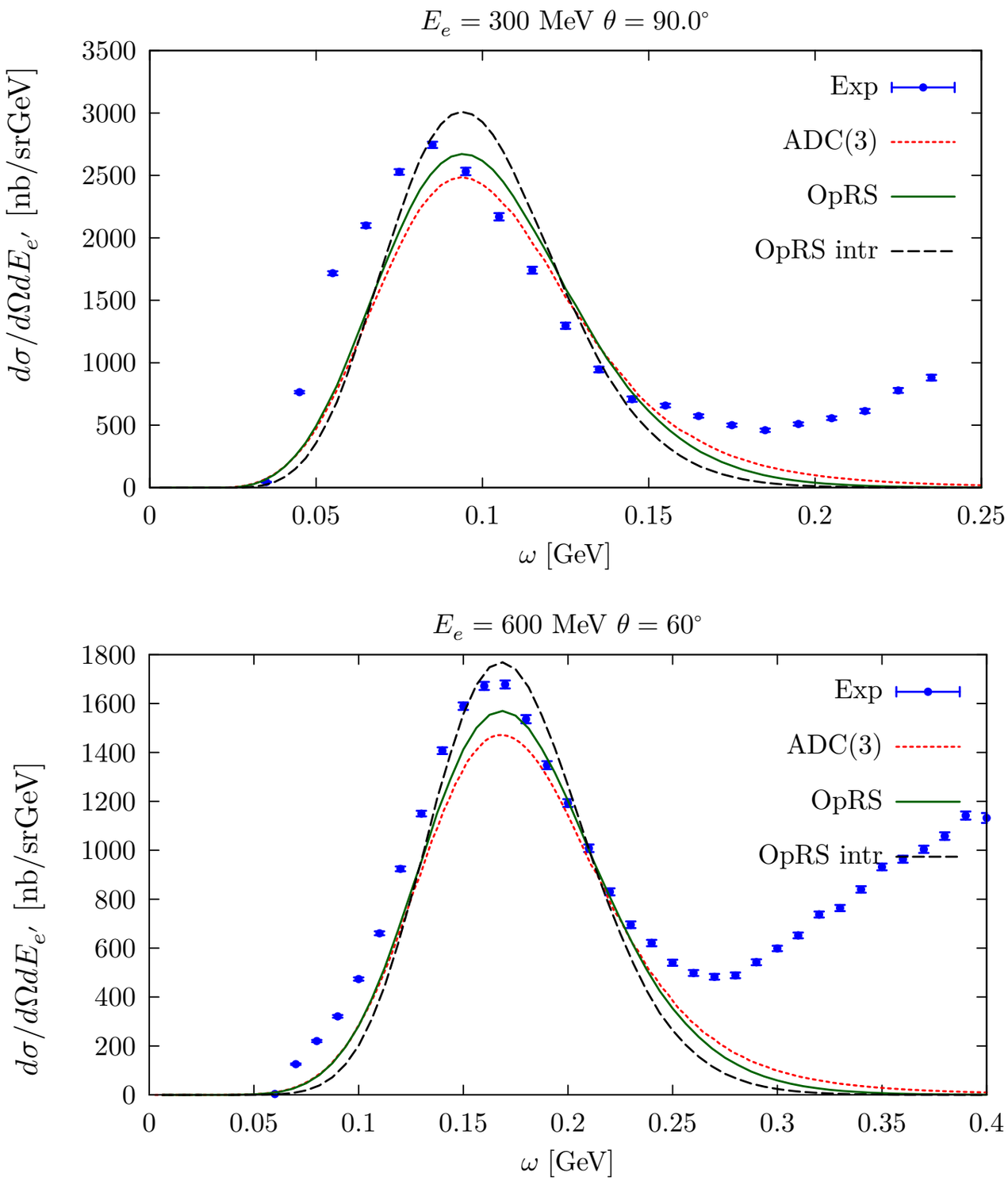





- Including FSI in the OpRS intrinsic results

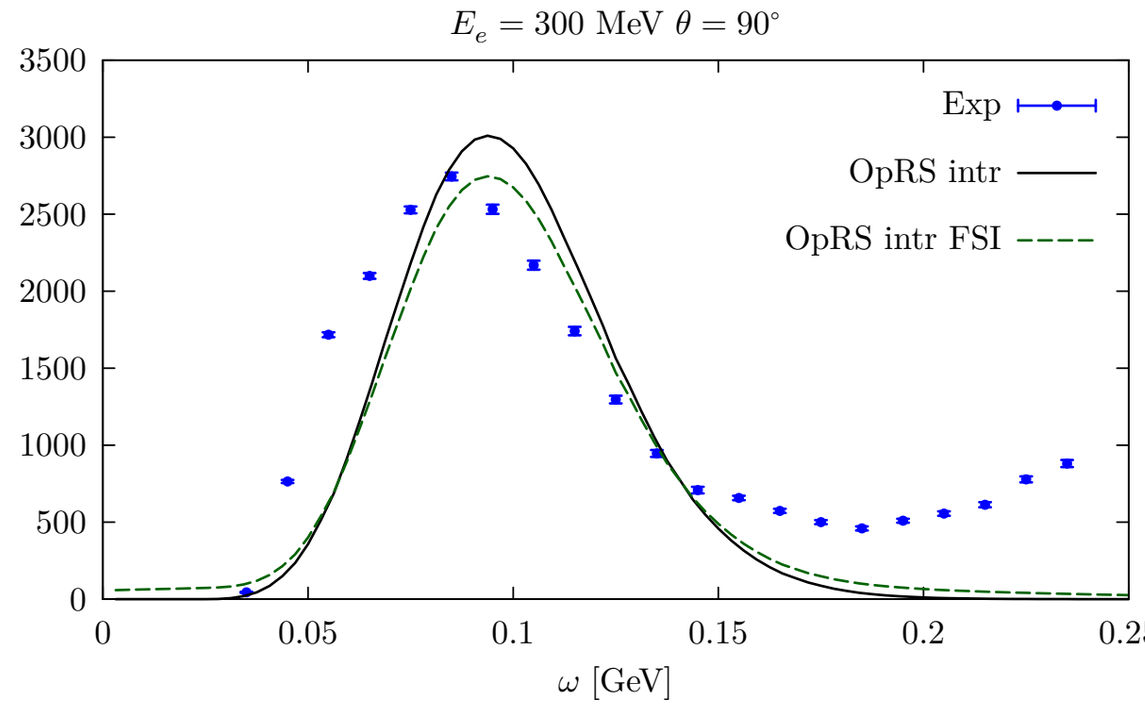


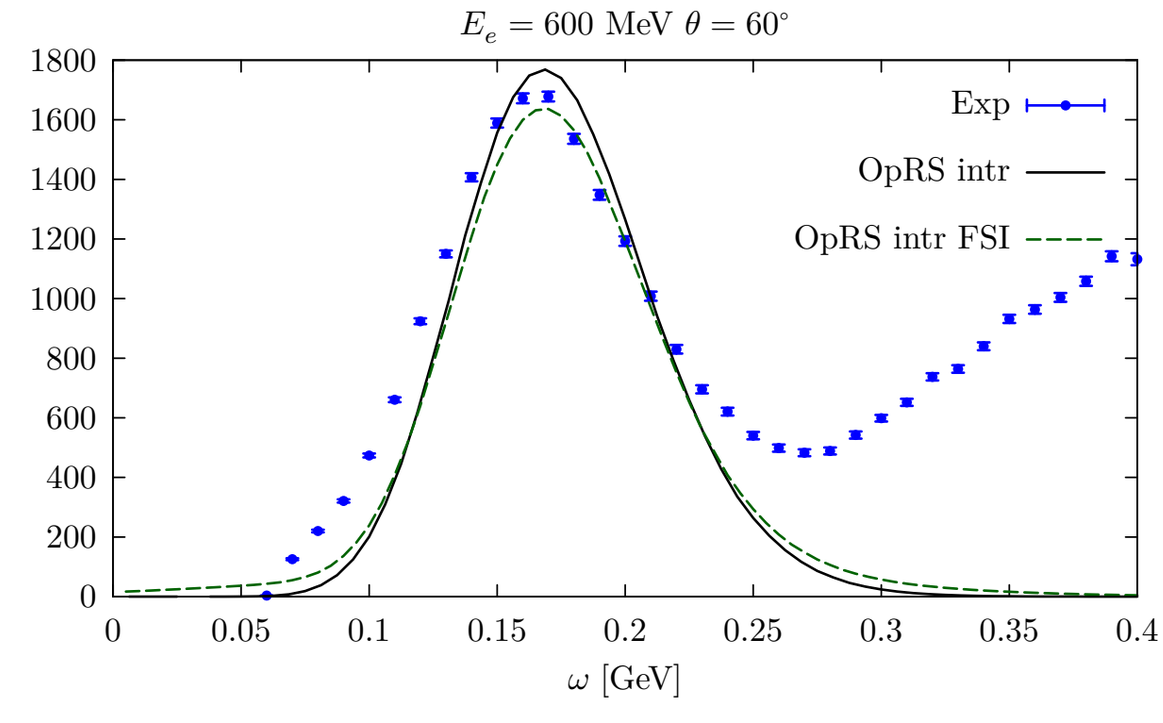

# $^{16}$O-e$^-$ cross sections within the SCGF approach

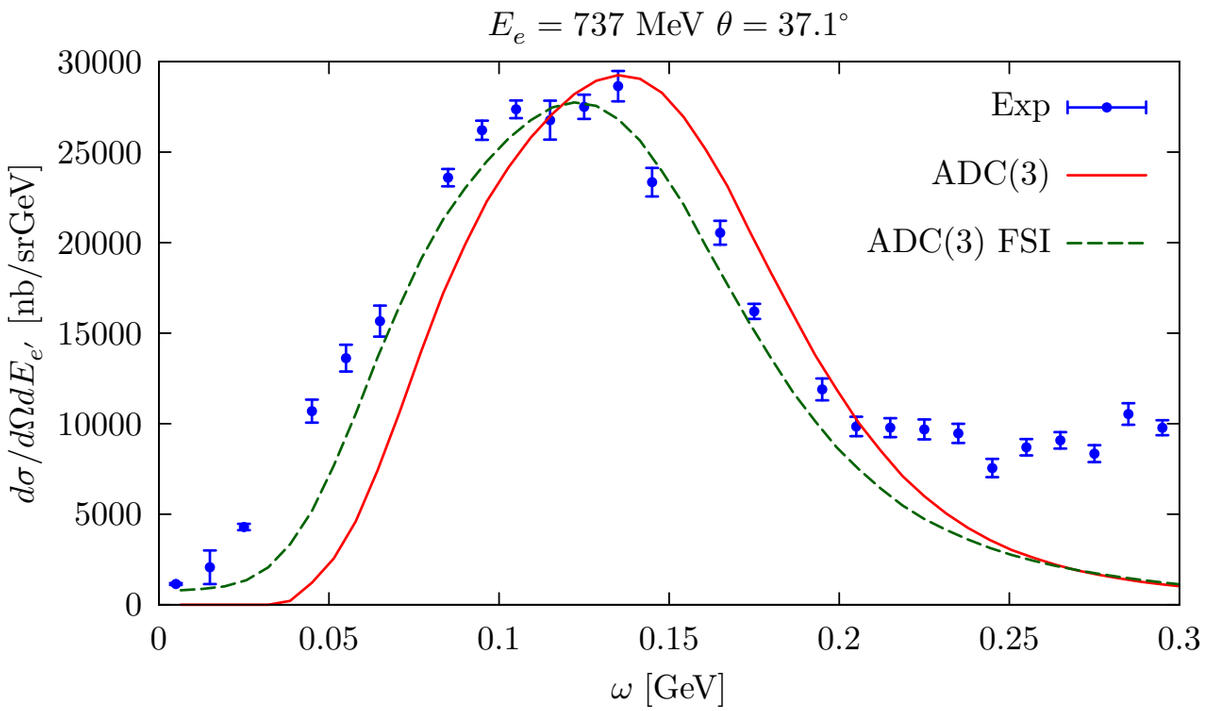


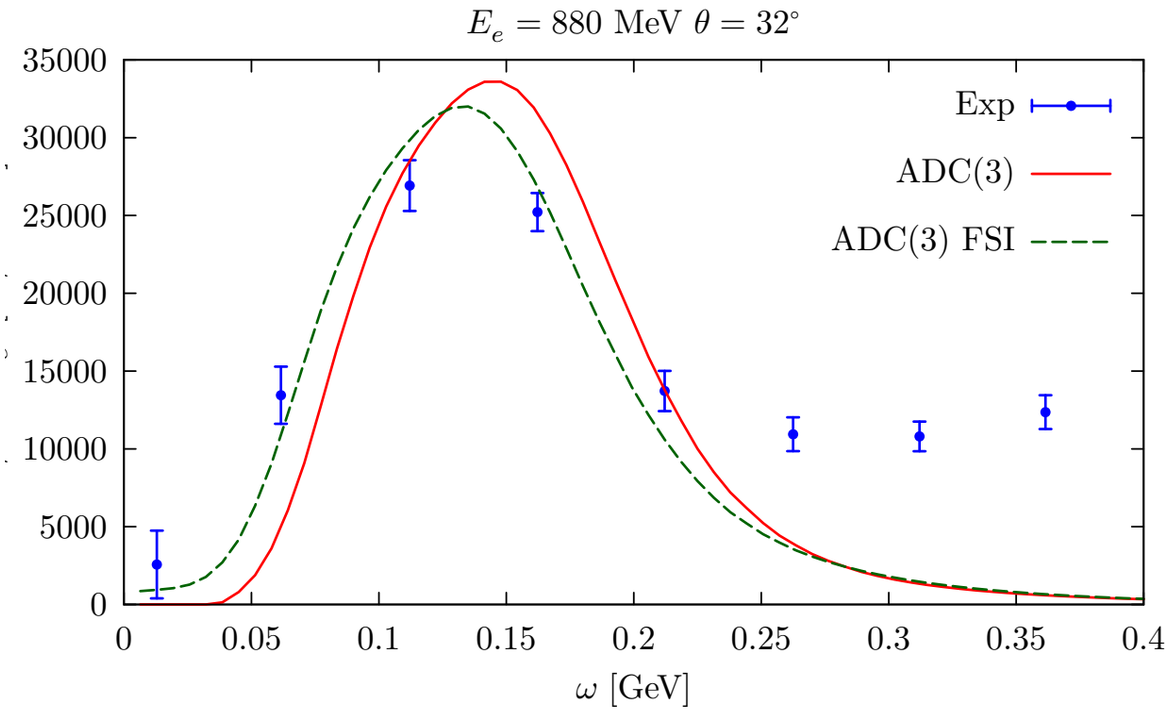


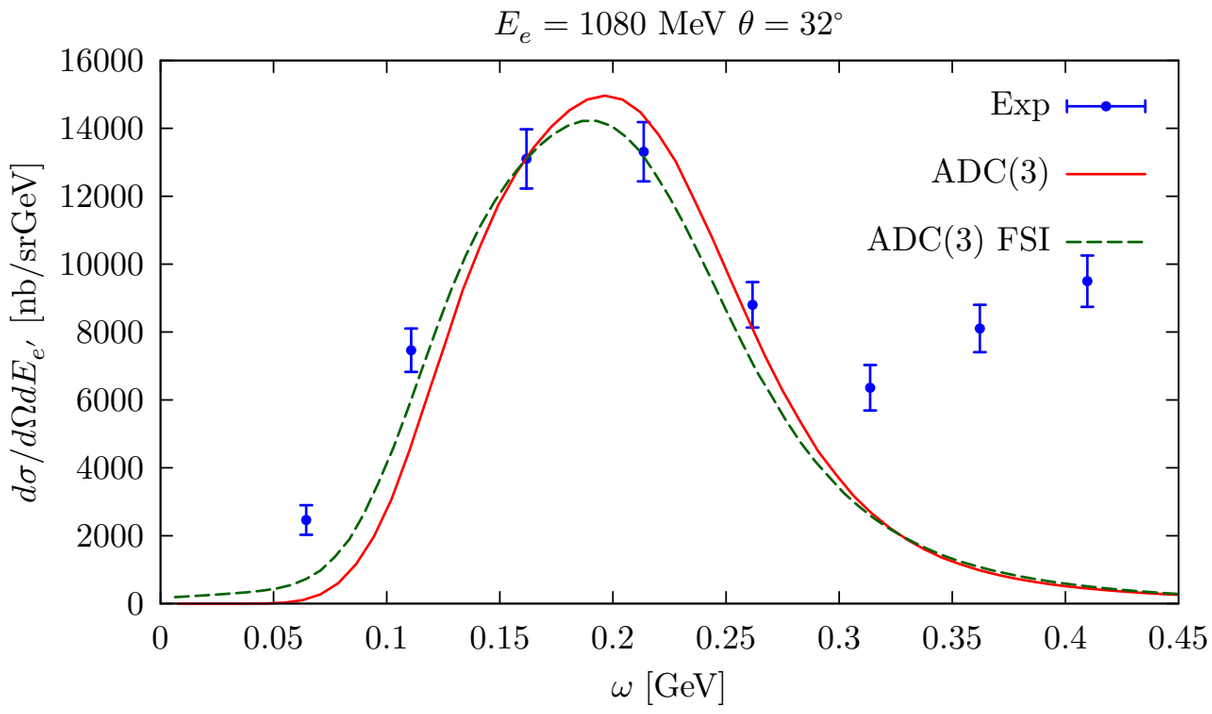


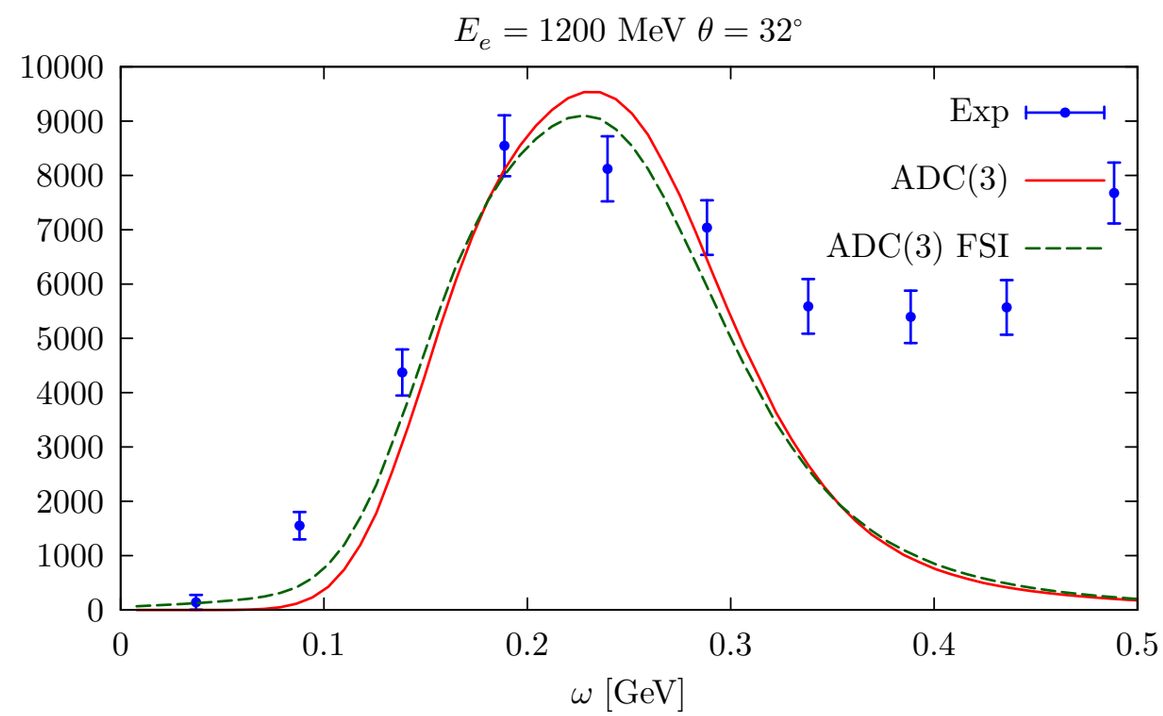

# The MiniBooNE CCQE (CC0π) puzzle

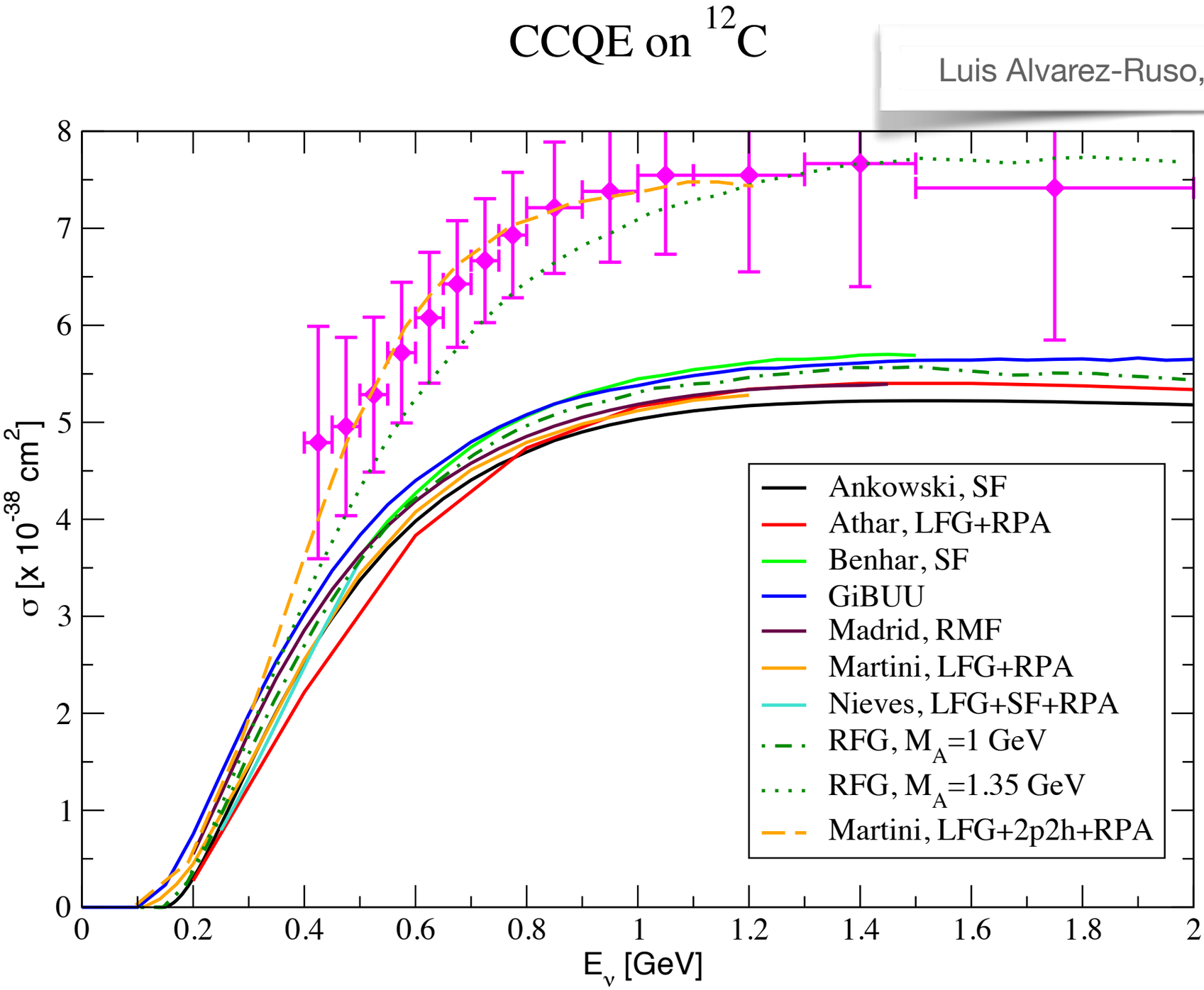


Luis Alvarez-Ruso, arXiv:1012.3871

- The 2p2h contribution is needed to explain the size of the measured cross section

# The CBF one-body Spectral Function of finite nuclei

- $^{12}$C Spectral Function obtained within CBF and using the Local Density Approximation

$$P_{LDA}(\mathbf{k},E) = P_{MF}(\mathbf{k},E) + P_{corr}(\mathbf{k},E)$$

$$\int d^3r P^{NM}_{corr}(\mathbf{k},E;\rho=\rho_A(r))$$

$$\sum_n Z_n |\phi_n(\mathbf{k})|^2 F_n(E-E_n)$$

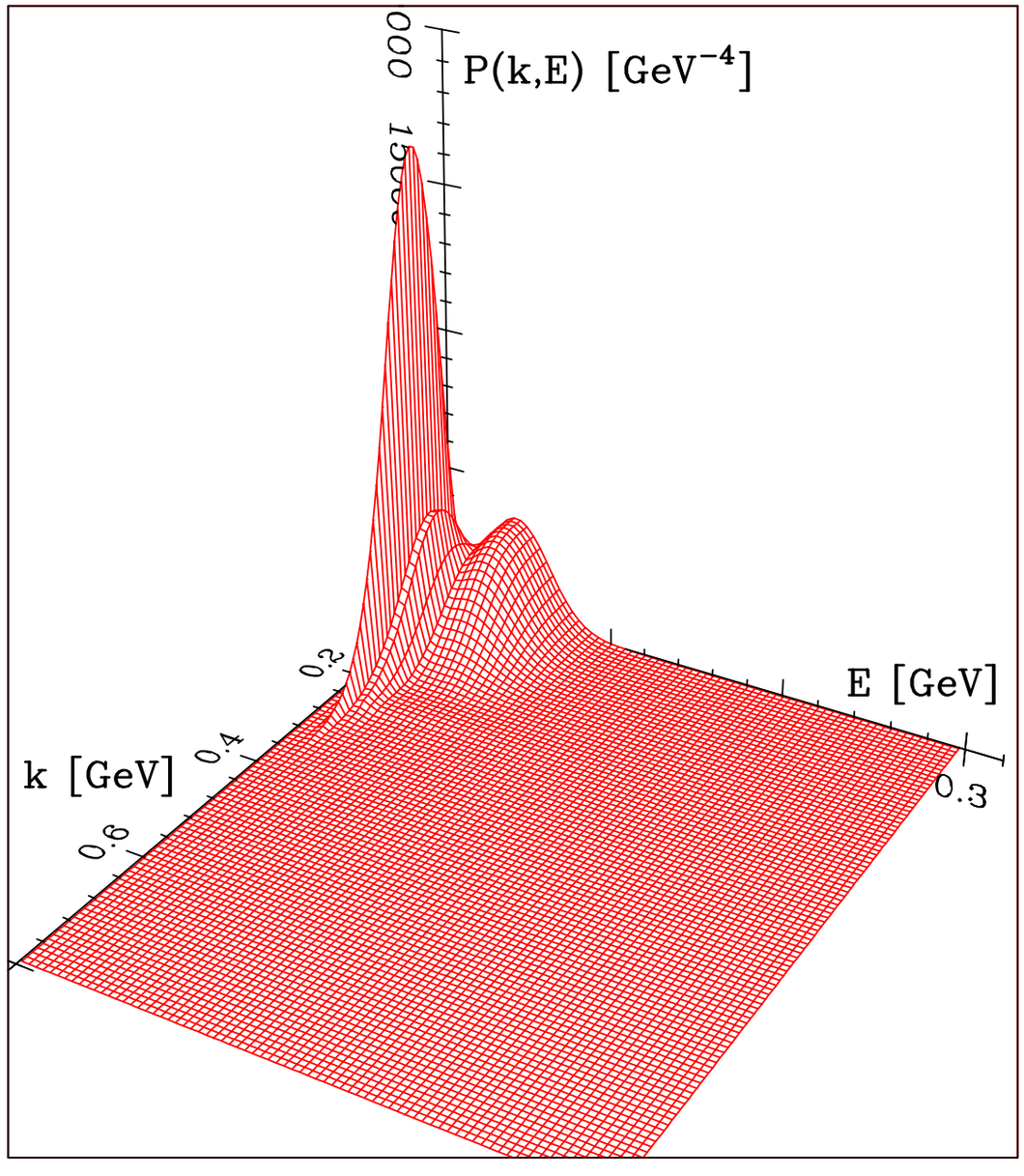


- $Z_n$ : spectroscopic factor extracted from (e, e'p)
- $F_n$ : finite width function accounting for residual interactions not included in a MF picture

- The one-body Spectral function of nuclear matter:

$$H = \sum_i \frac{\mathbf{p}_i^2}{2m} + \sum_{i<j} v_{ij} + \sum_{i<j<k} V_{ijk}$$

Argonne v18

UIX, IL7

# Production of two particle-two hole (2p2h) states

- Initial State Correlations

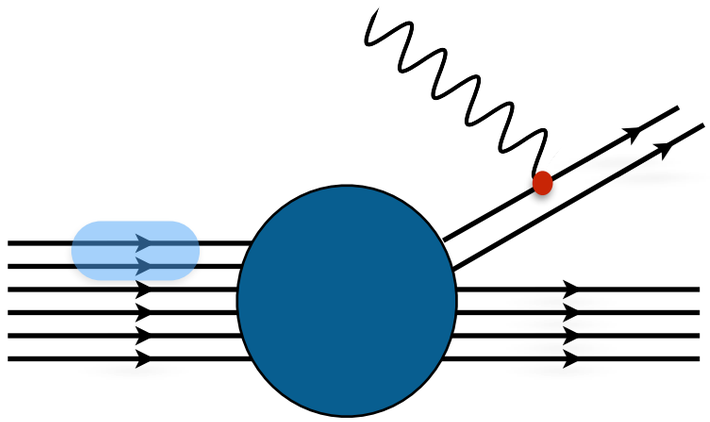

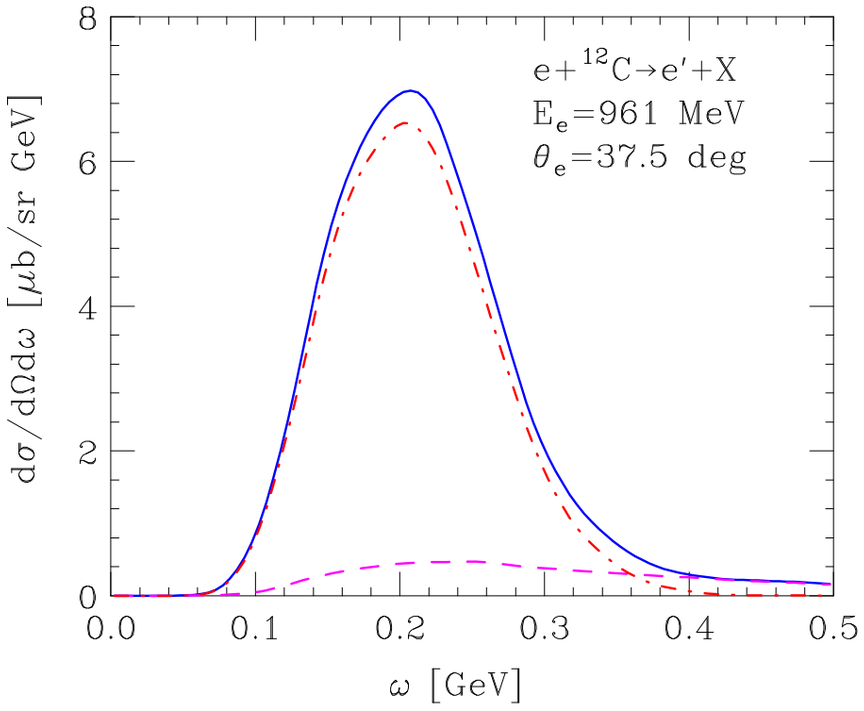


- $P_{corr}(\mathbf{k},E)$ accounts for the presence of strongly correlated pairs. Its contribution to the cross section is clearly visible: appearance of a tail in the large energy transfer region

- The Impulse Approximation is adopted

$$d\sigma_A = \int dE\, d^3k\, d\sigma_N P(\mathbf{k}, E)$$

# Production of two particle-two hole (2p2h) states

- Initial State Correlations

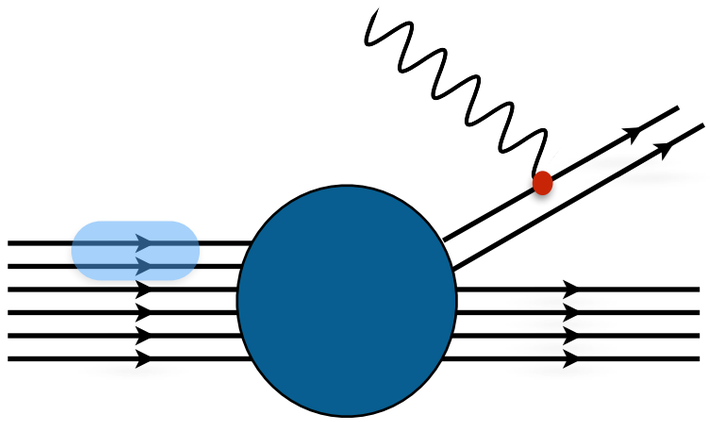

+

- Meson Exchange currents

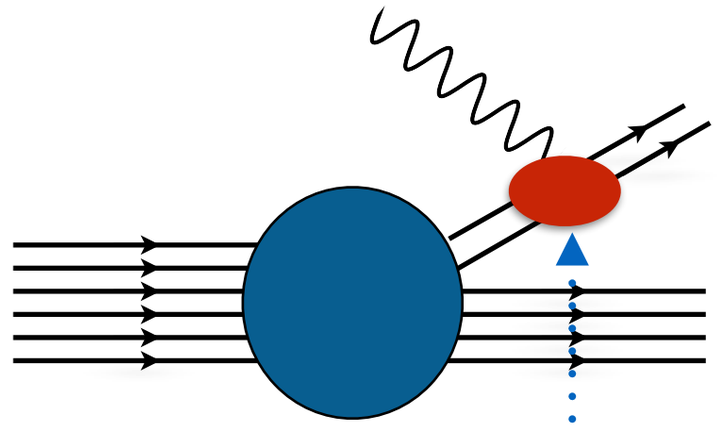

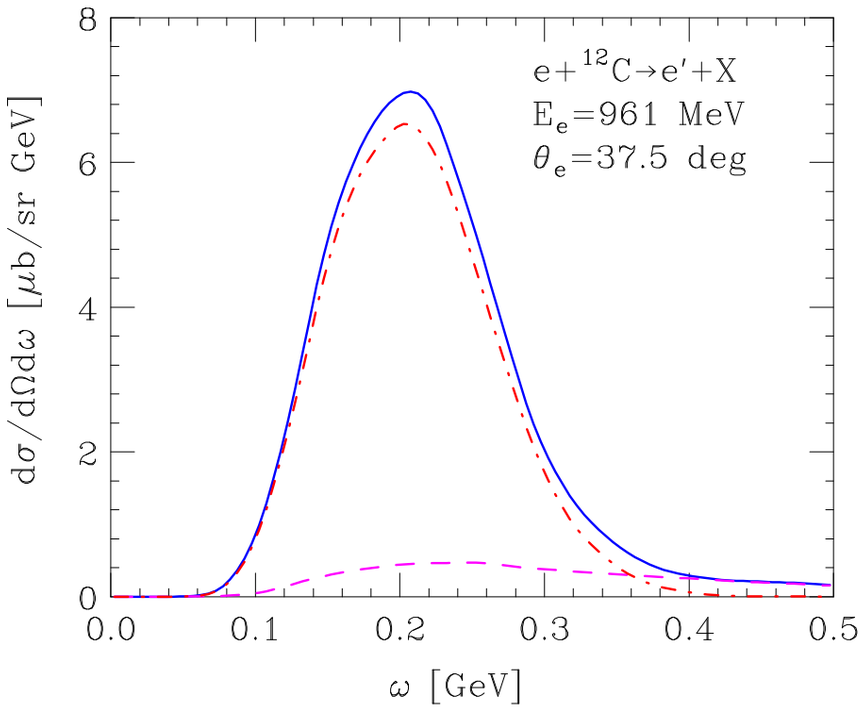


- $P_{corr}(\mathbf{k},E)$ accounts for the presence of strongly correlated pairs. Its contribution to the cross section is clearly visible: appearance of a tail in the large energy transfer region

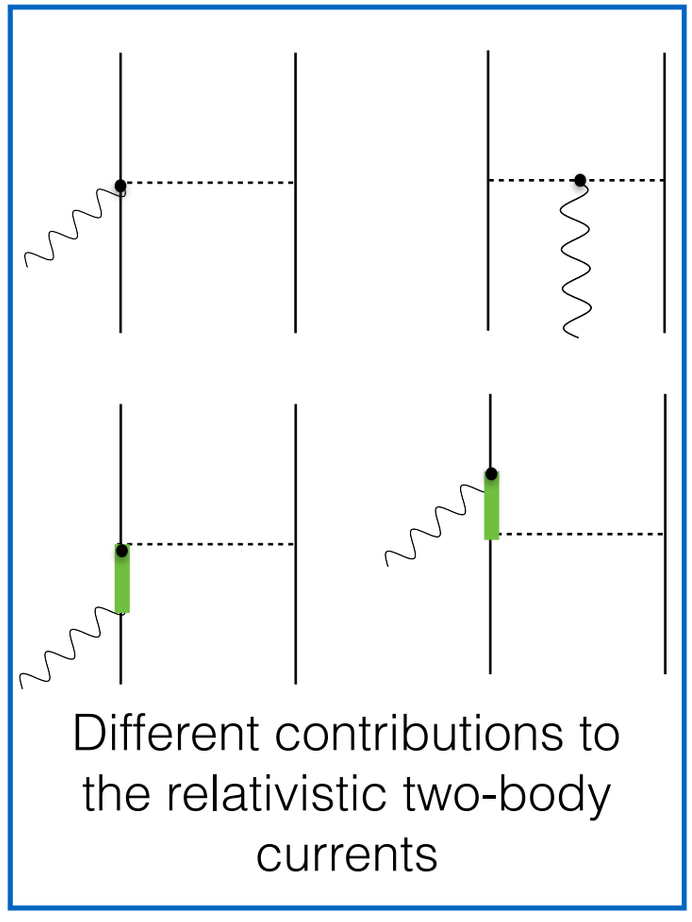

Different contributions to the relativistic two-body currents

# Production of two particle-two hole (2p2h) states

- Initial State Correlations

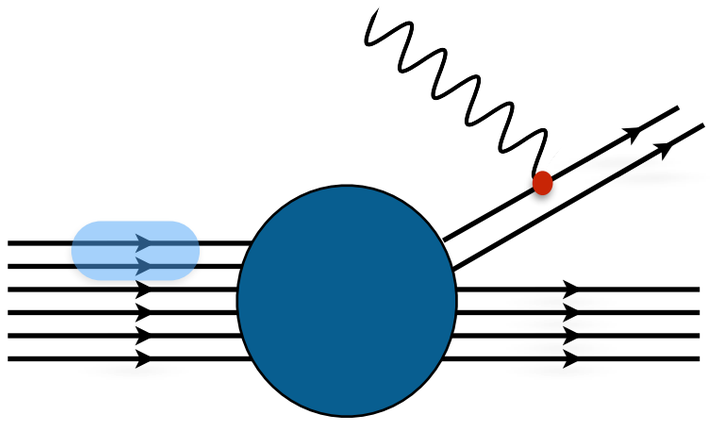

+

- Meson Exchange currents

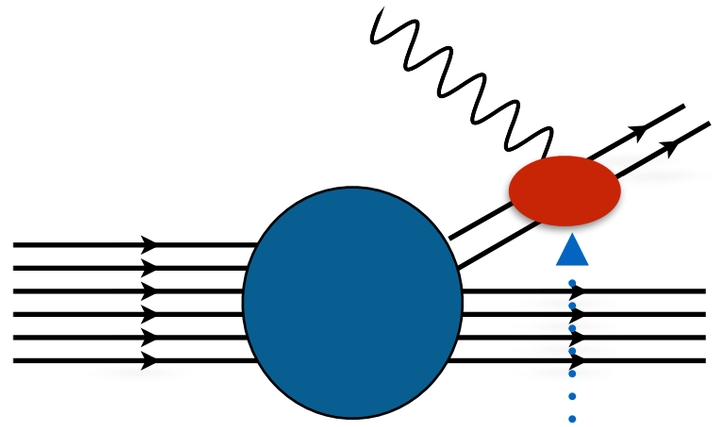

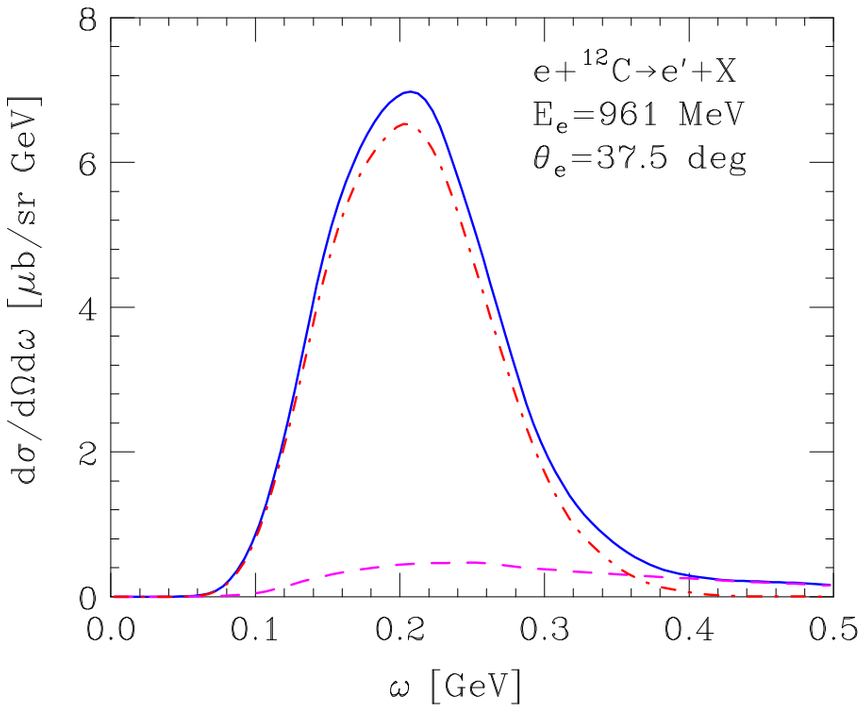


- $P_{corr}(\mathbf{k},E)$ accounts for the presence of strongly correlated pairs. Its contribution to the cross section is clearly visible: appearance of a tail in the large energy transfer region

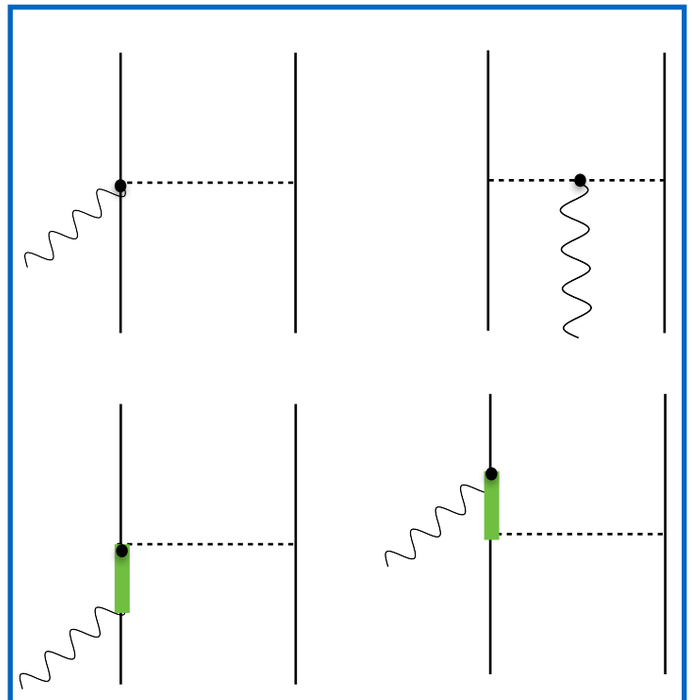

Different contributions to the relativistic two-body currents

- The Impulse Approximation has been generalized:

$$W^{\mu\nu}_{2p2h} = W^{\mu\nu}_{ISC} + W^{\mu\nu}_{MEC} + W^{\mu\nu}_{int}$$

# Results for electron-$^{12}$C cross sections

- Separate contributions: IA

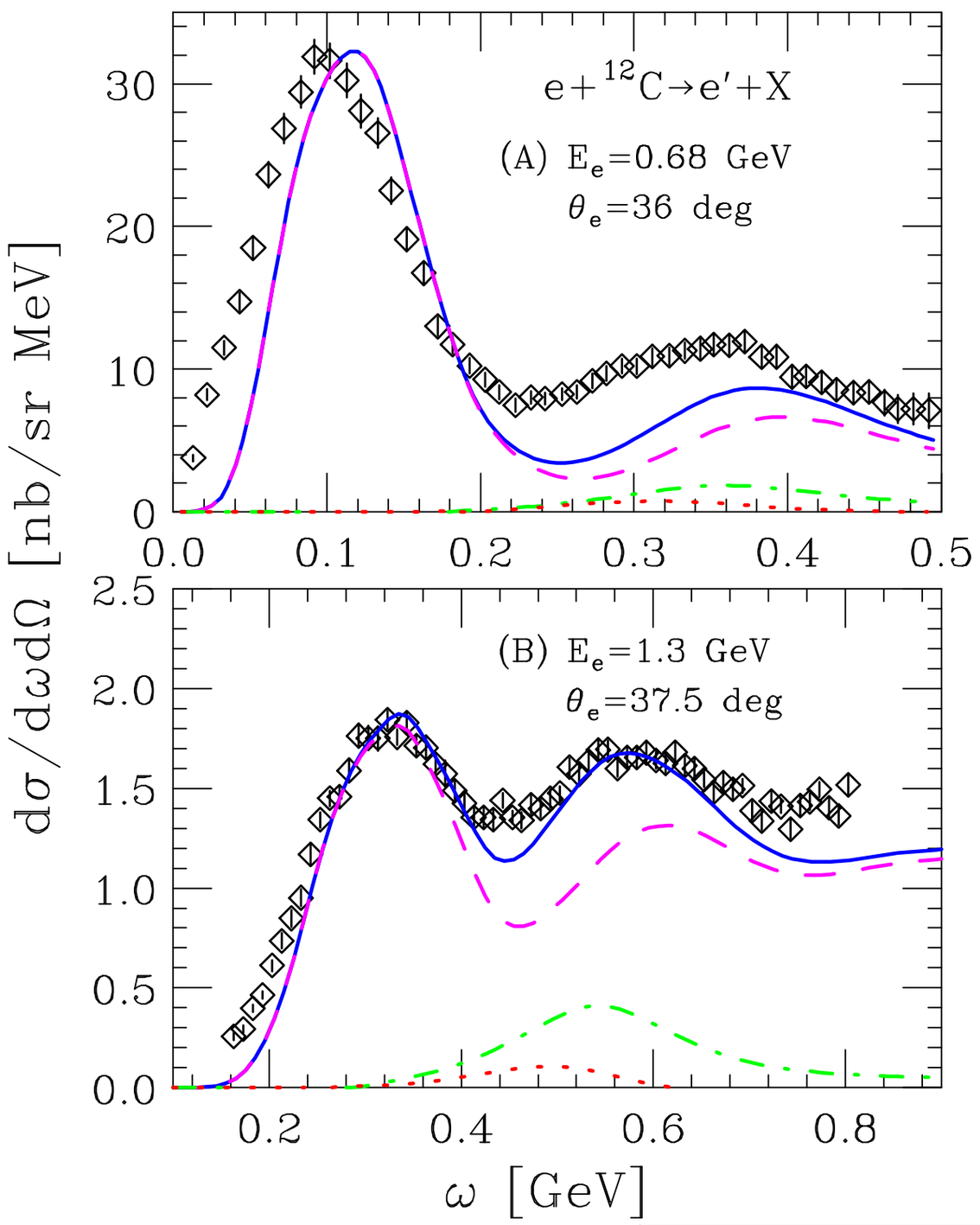


- Including FSI in the QE region

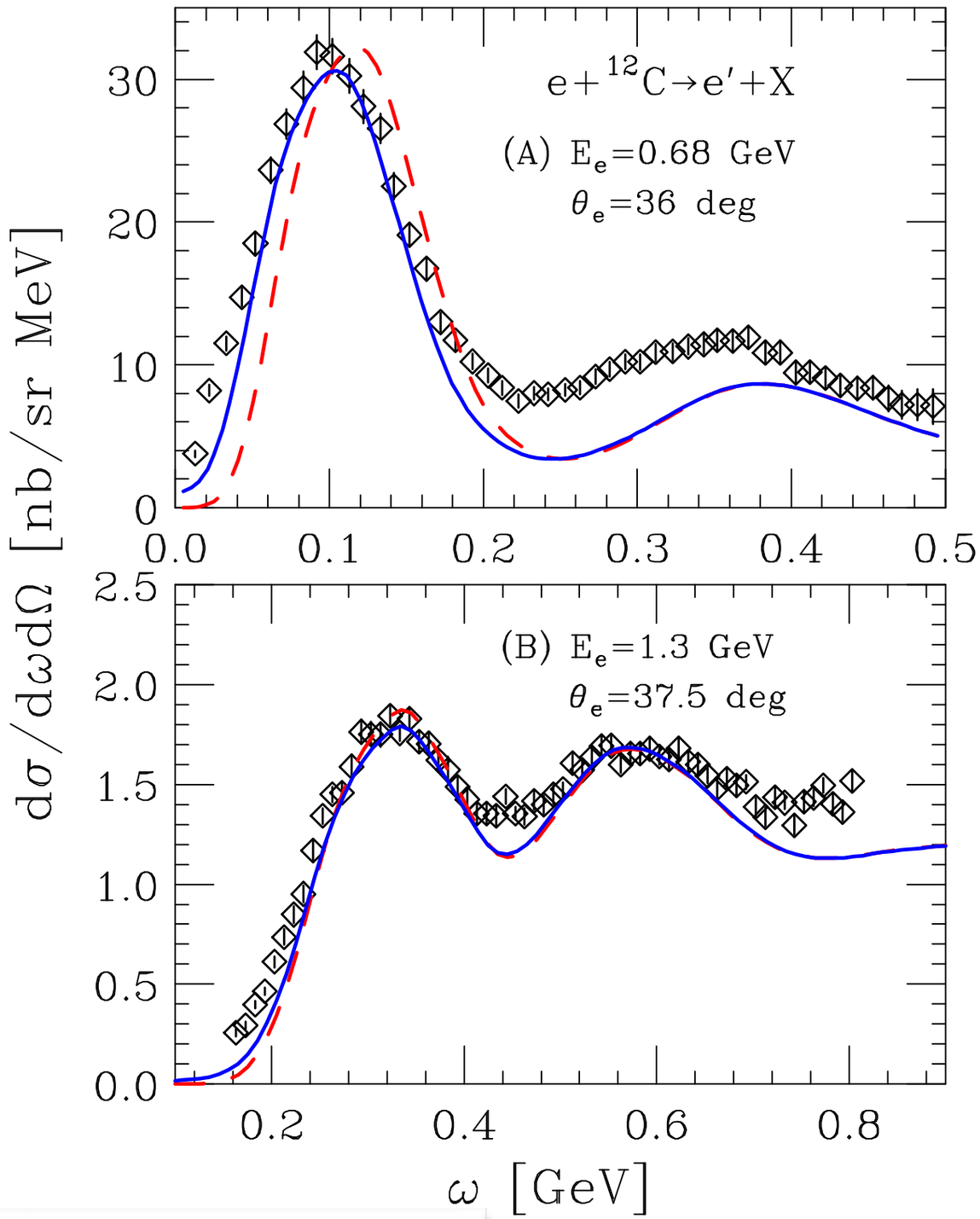


NR, A.Lovato, O.Benhar, PRL 116, 192501 (2016)

# (Anti)neutrino -$^{12}$C scattering cross sections

The inclusive cross section of the process in which a neutrino or antineutrino scatters off a nucleus can be written in terms of five response functions

$$\frac{d\sigma}{dE_{\ell'}d\Omega_\ell} \propto [v_{00}R_{00} + v_{zz}R_{zz} - v_{0z}R_{0z} + v_{xx}R_{xx} \mp v_{xy}R_{xy}]$$

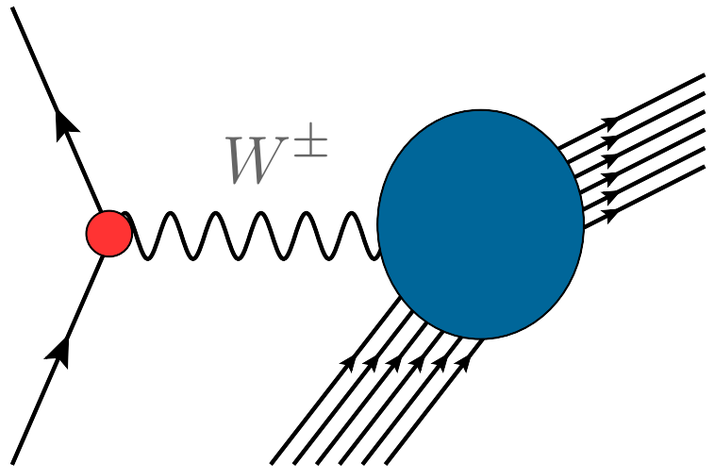


- The two-body diagrams contributing to the axial and vector responses

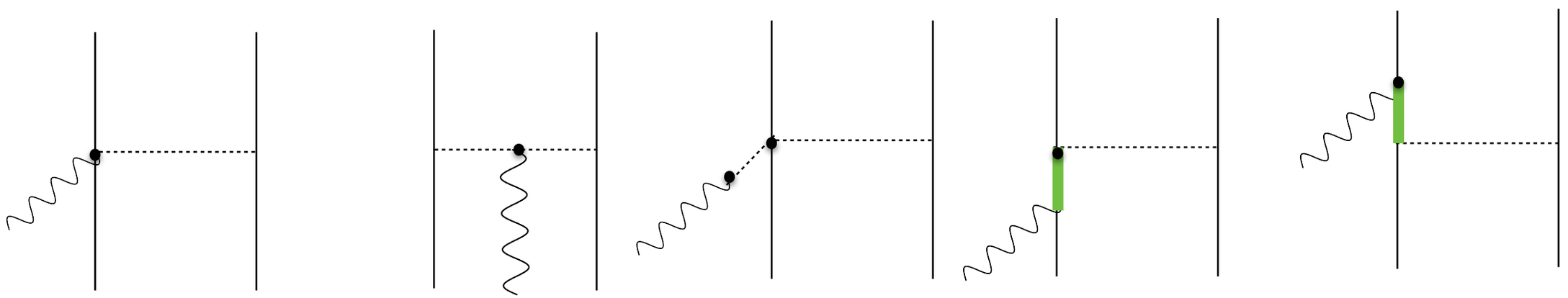

- In the preliminary results we present we only included:

$$W^{\mu\nu}_{2p2h} = W^{\mu\nu}_{ISC} + W^{\mu\nu}_{MEC} + \cancel{W^{\mu\nu}_{int}}$$

# Two-body CC response functions of $^{12}C$

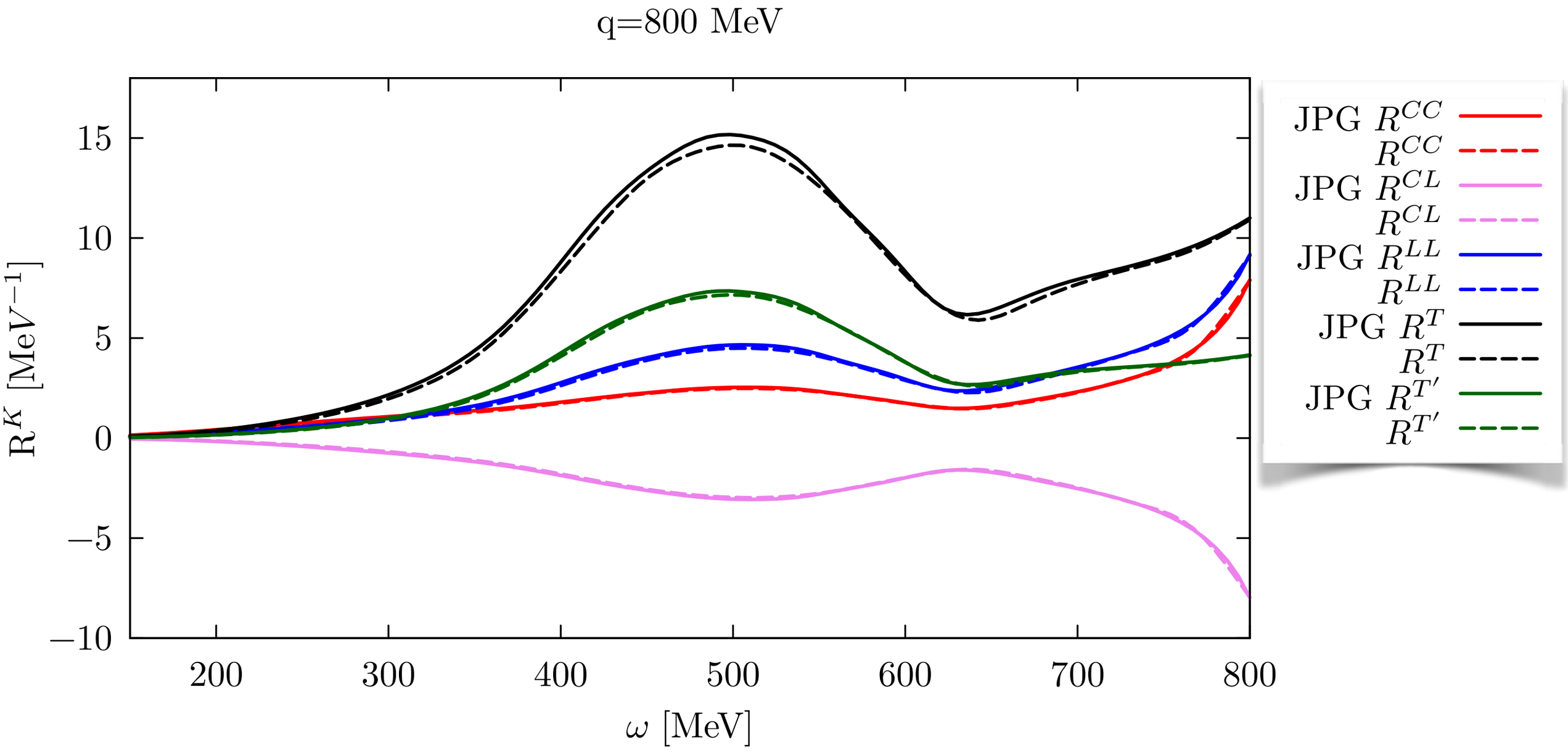


- Comparison of the five CC response functions of $^{12}C$ with the results of I. Ruiz Simo, et. al, Journal of Phys. G 44, no. 6 (2017). The different curves have been obtained with the GRFG model

# CC0π neutrino - $^{12}$C cross sections

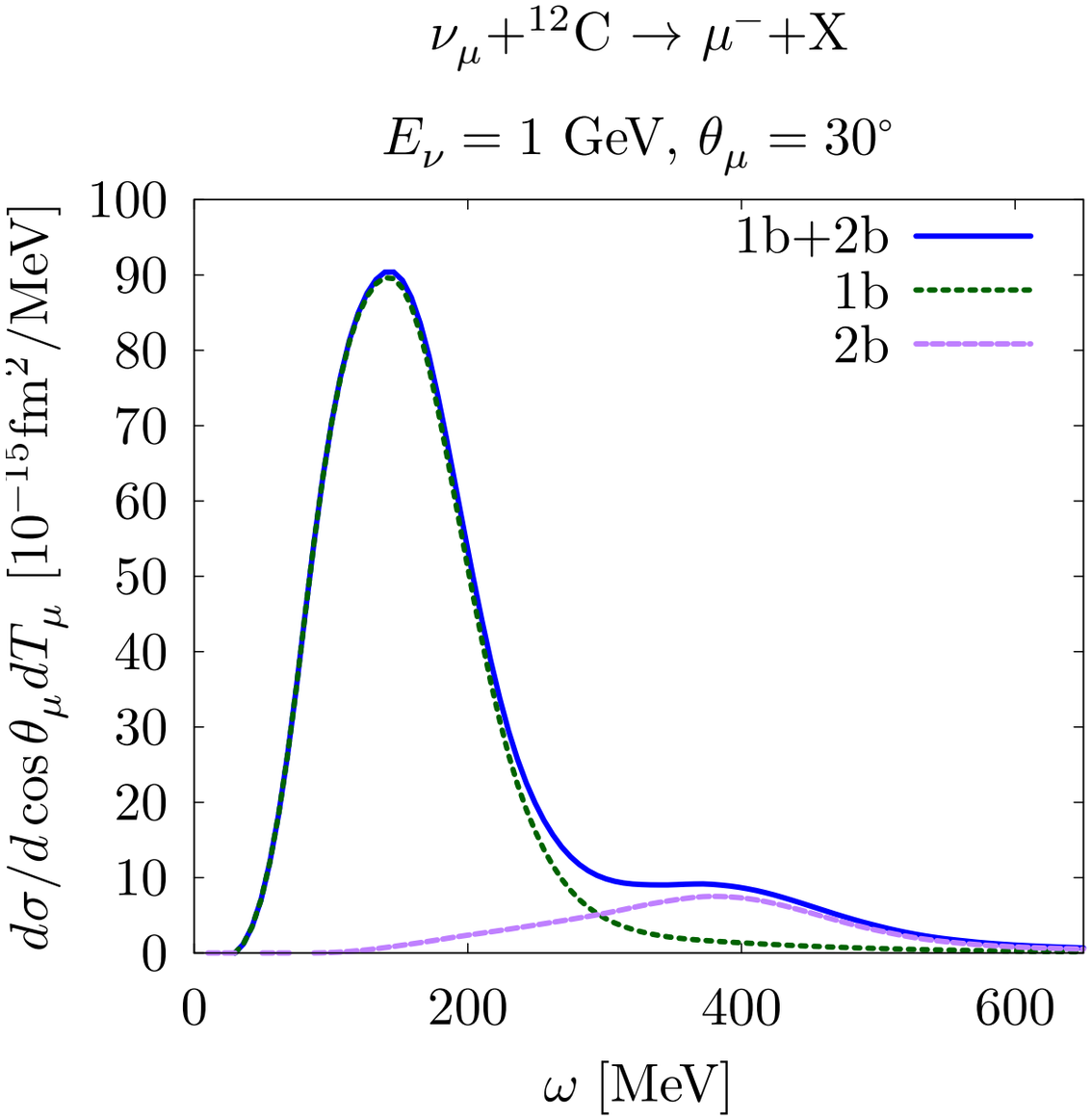


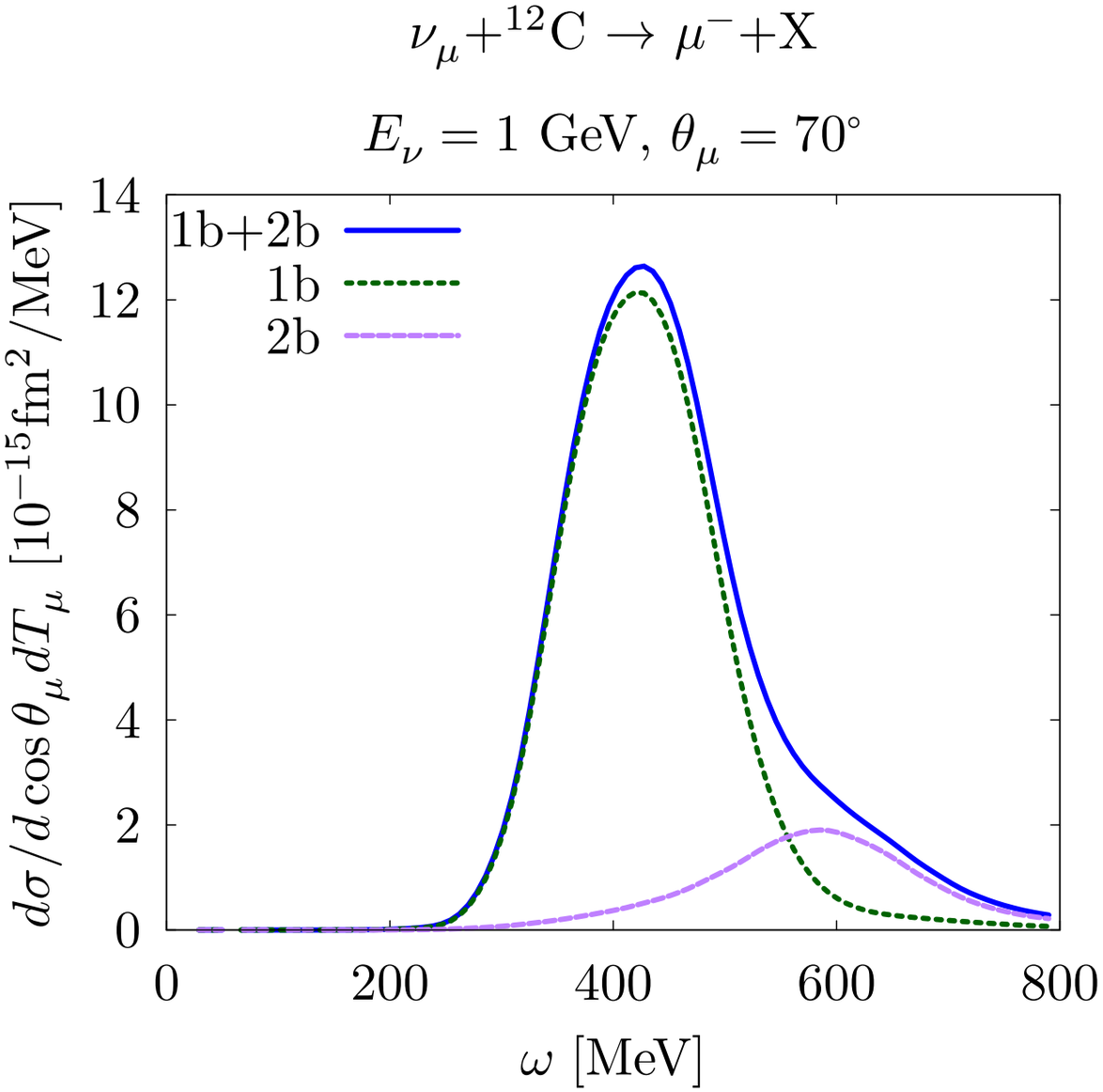


- The 2b contribution mostly affects the ‘dip’ region, in analogy with the electromagnetic case

- Meson exchange currents strongly enhance the cross section for large values of the scattering angle

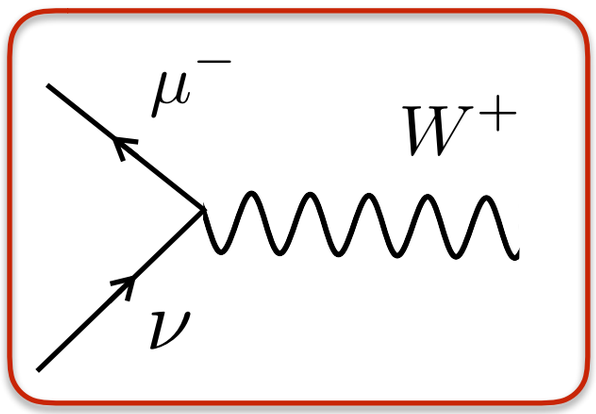

# CC0π antineutrino - $^{12}$C cross sections

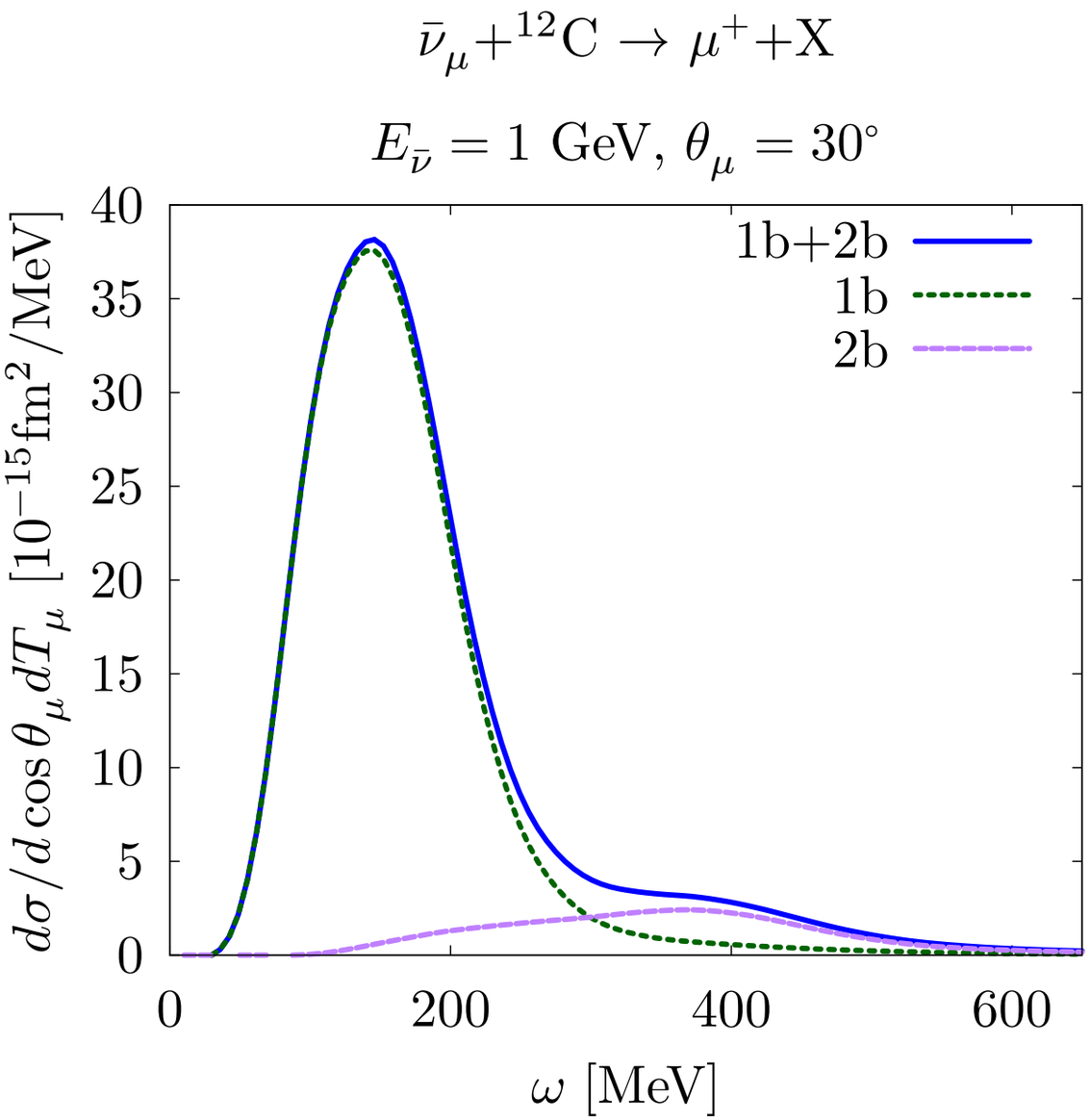


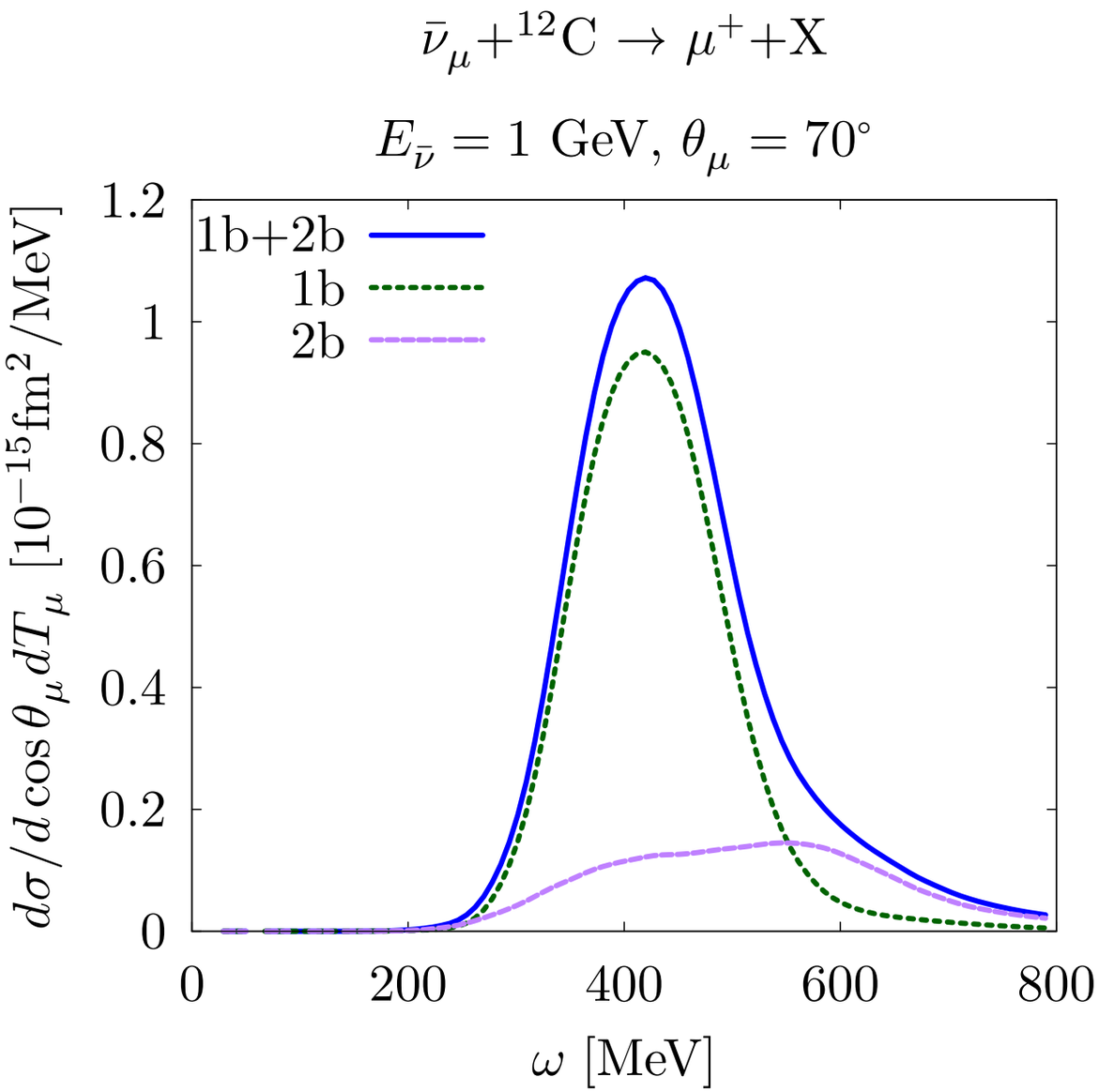


- The 2b contribution mostly affects the ‘dip’ region, in analogy with the electromagnetic case
- Meson exchange currents strongly enhance the cross section for large values of the scattering angle

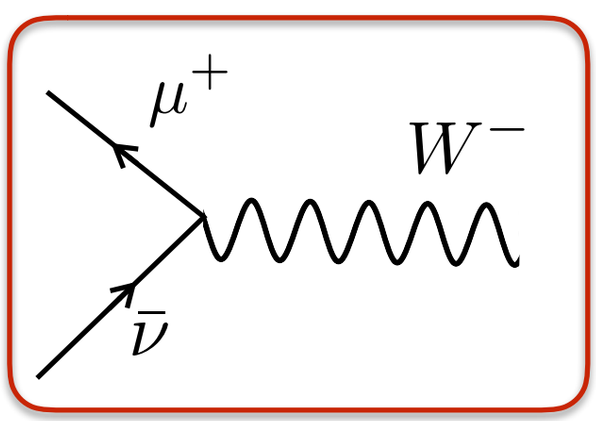

# NC0π neutrino - $^{12}$C cross sections

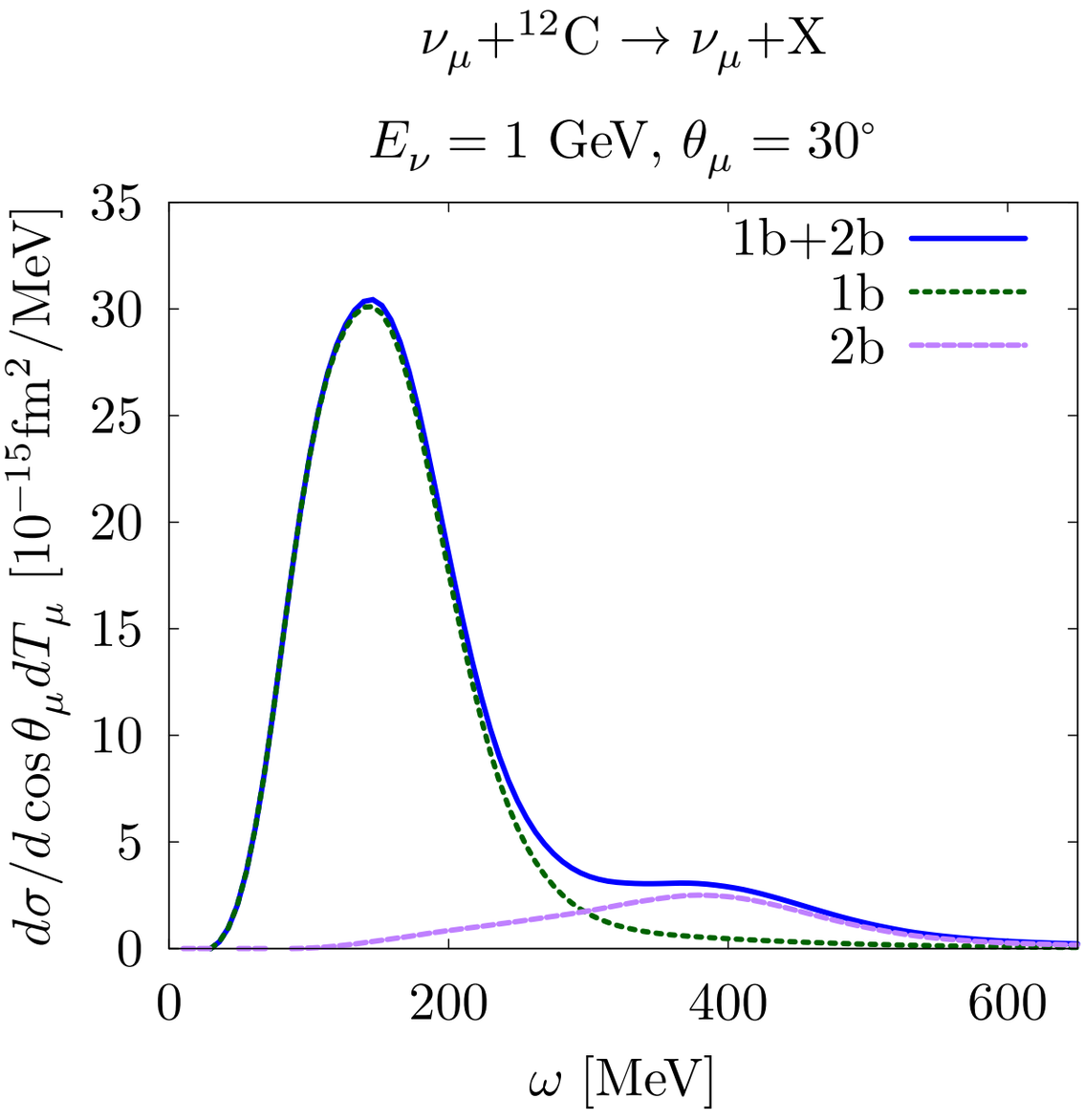


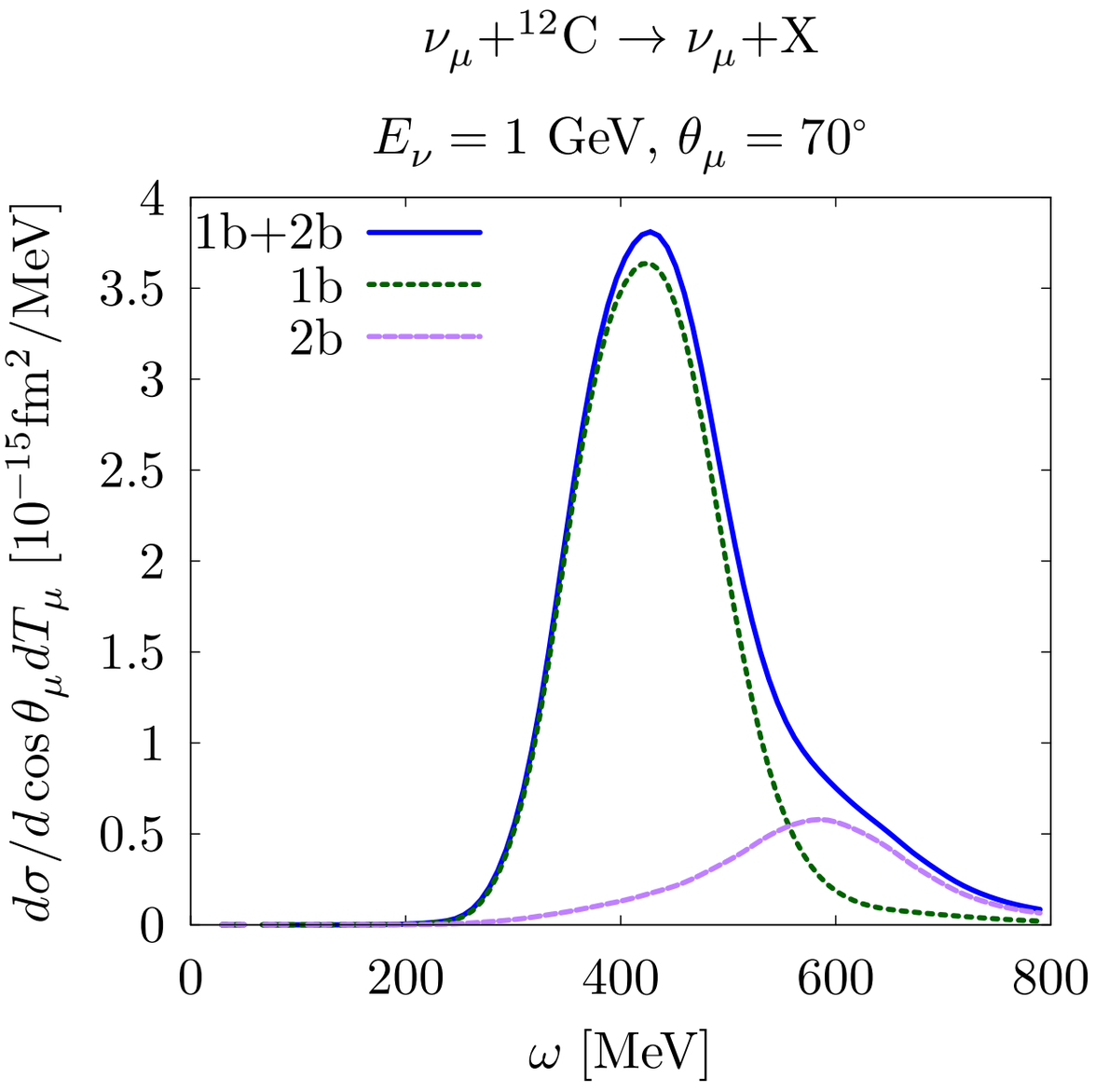


- The 2b contribution mostly affects the ‘dip’ region, in analogy with the electromagnetic case
- Meson exchange currents strongly enhance the cross section for large values of the scattering angle

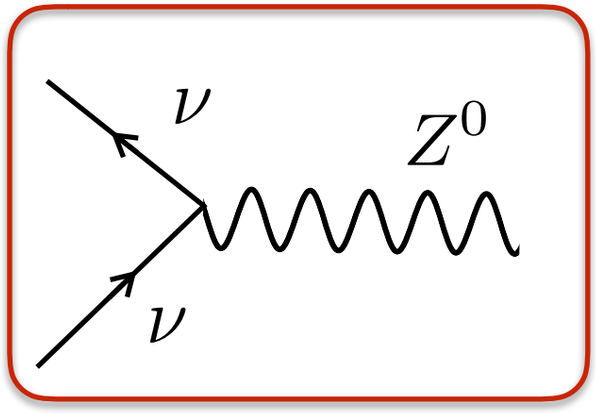

# NC0π antineutrino - $^{12}$C cross sections

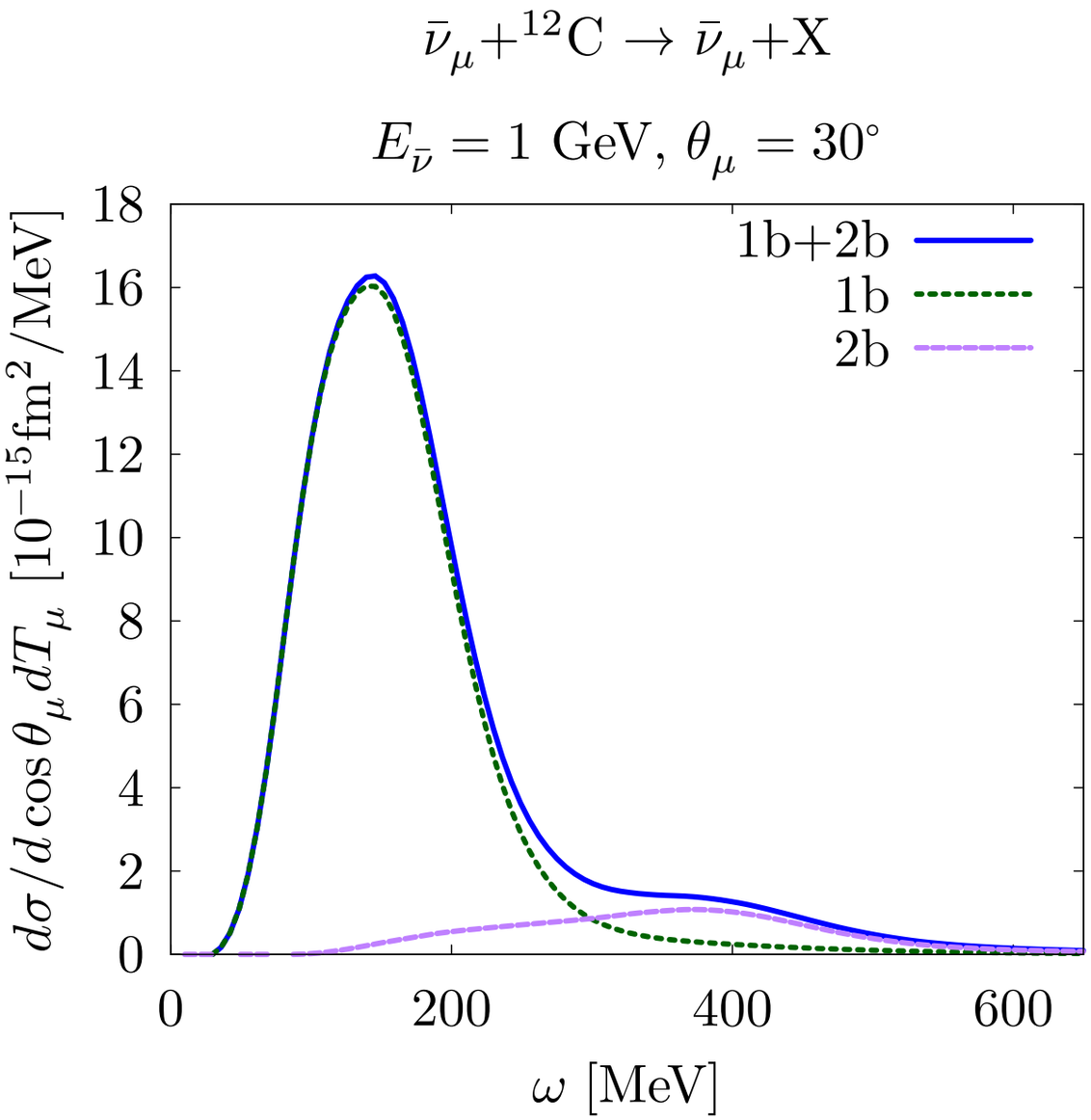


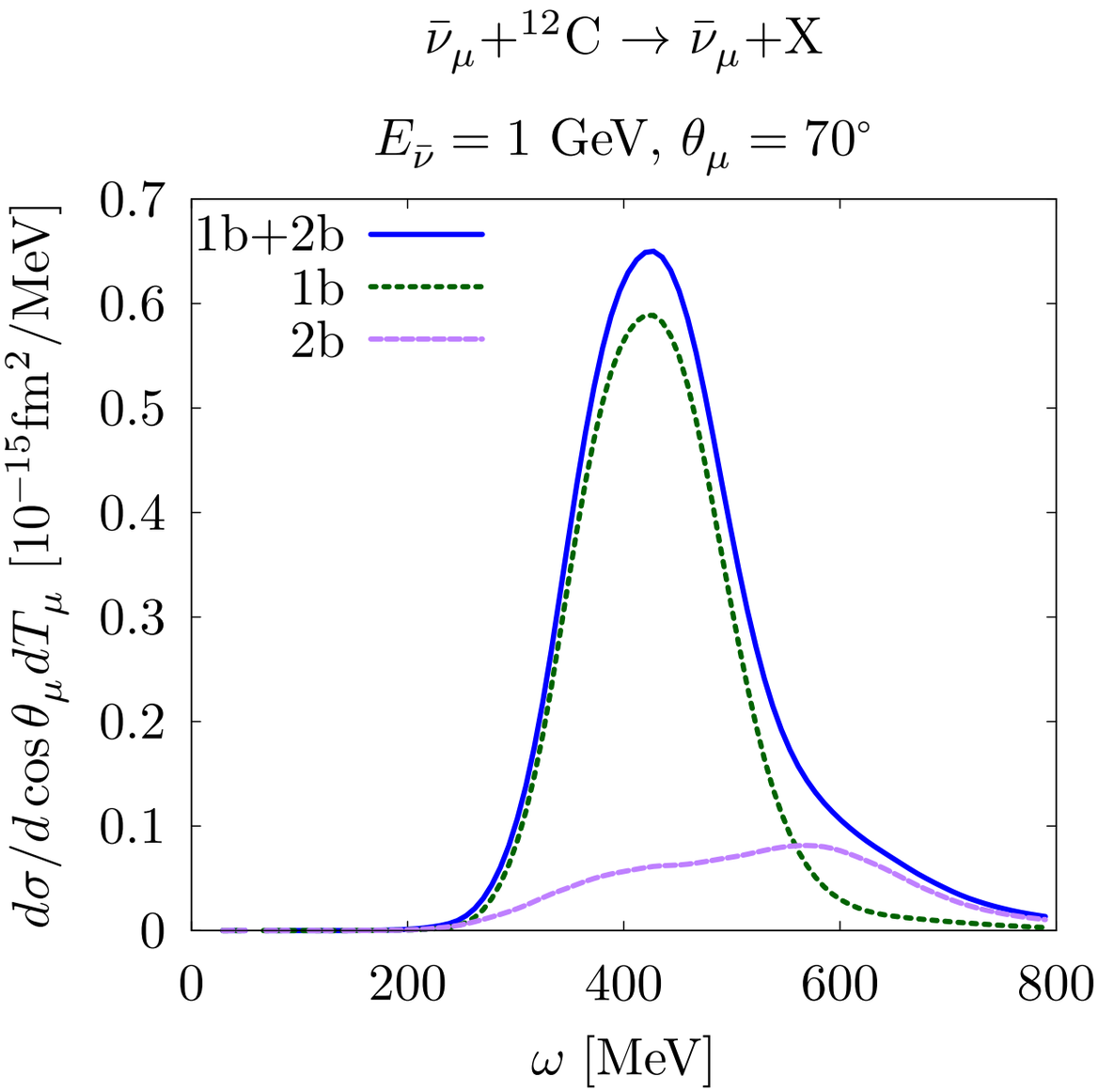


- The 2b contribution mostly affects the ‘dip’ region, in analogy with the electromagnetic case
- Meson exchange currents strongly enhance the cross section for large values of the scattering angle

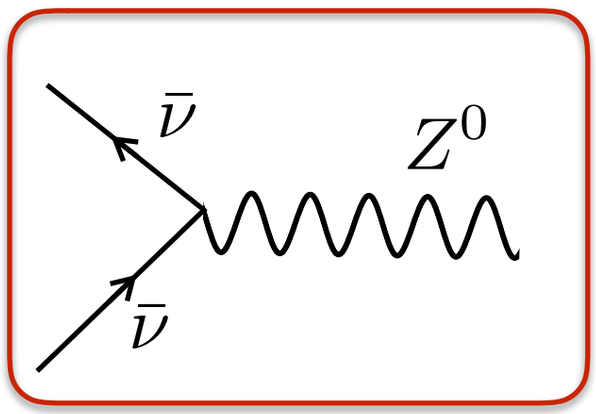

# CC0π total cross section: MiniBooNE data

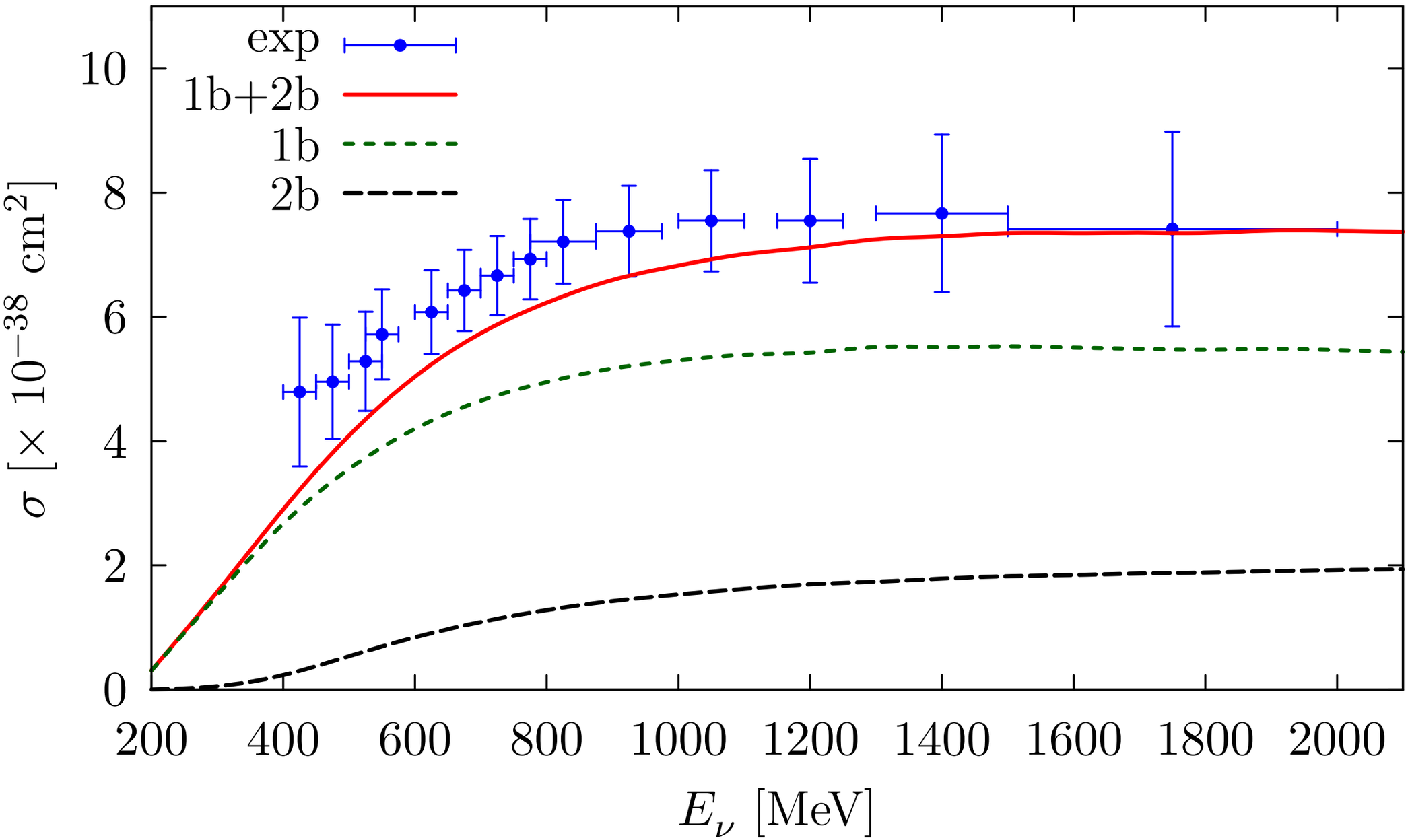


- The 2p2h contribution is needed to explain the size of the measured cross section

# Prospects

- Green's Function Monte Carlo approach :
  - ❖ Extend the interpolation algorithm and the two-body fragment model to describe the NC0π inclusive cross section
  - ❖ Spectral Function calculation of light nuclei within GFMC with both phenomenological and chiral Hamiltonians
- Self Consistent Green's Function approach :
  - ❖ Extension to the electroweak sector including both one- and two-body currents for closed shell nuclei
  - ❖ The SCGF method has recently been reformulated within the Gorkov's theory that allows to tackle open shell nuclei. Provide predictions for electron and neutrino scattering on $^{40}$Ar and $^{48}$Ti
- Correlated Basis Function
  - ❖ Flux-folded double differential inclusive cross sections for CC0π and NC0π processes
  - ❖ Inclusion of the interference between one- and two-body currents: benchmark with GFMC

# Back up slides

# Relativistic effects in a correlated system

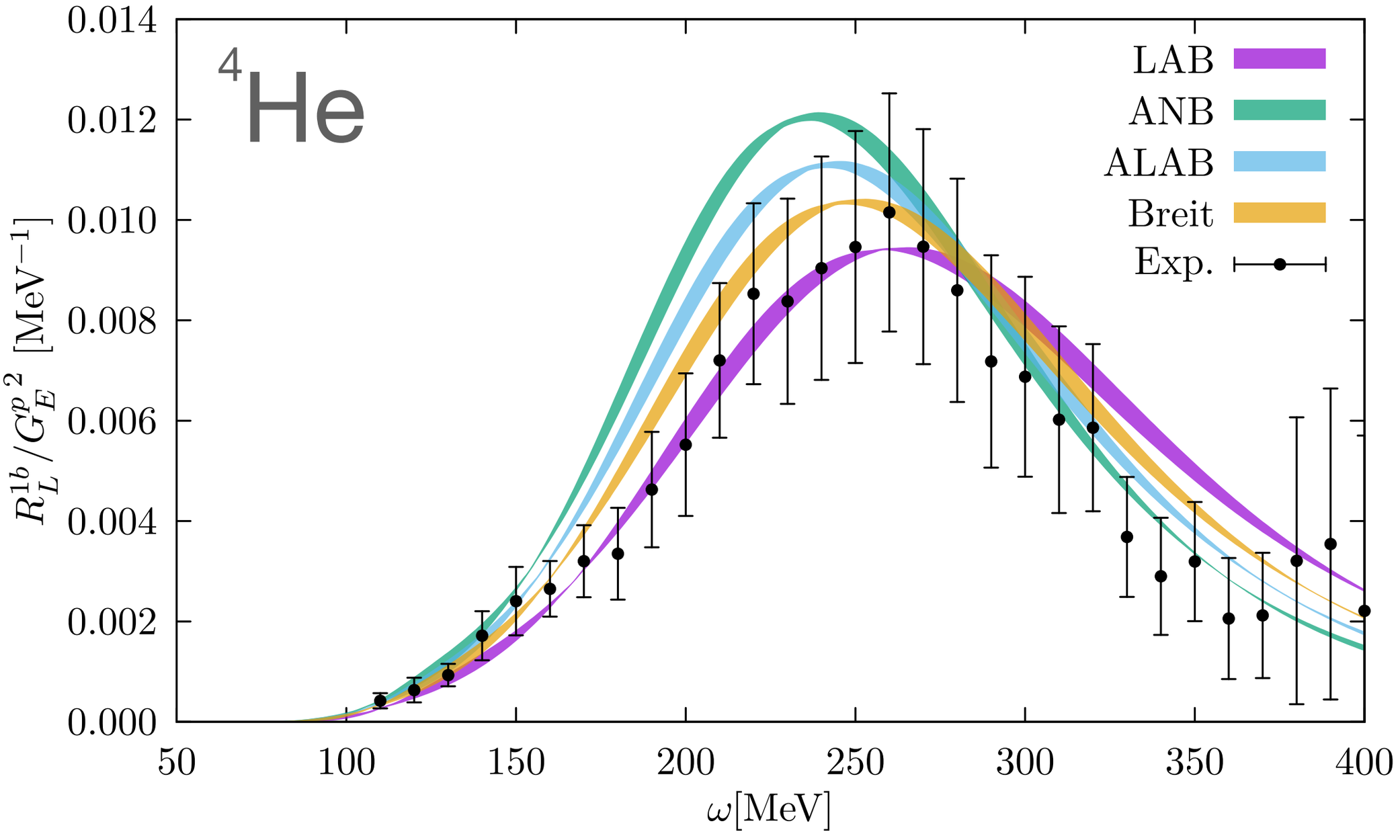


- Longitudinal responses of $^4$He for |q|=700 MeV in the four different reference frames. The curves show differences in both peak positions and heights.

# Relativistic effects in a correlated system

- The frame dependence can be drastically reduced if one assumes a two-body breakup model with relativistic kinematics to determine the input to the non relativistic dynamics calculation

$$p^{fr} = \mu\left(\frac{p_N^{fr}}{m_N} - \frac{p_X^{fr}}{M_X}\right) \qquad \mu = \frac{m_N M_X}{m_N + M_X}$$

$$P_f^{fr} = p_N^{fr} + p_X^{fr}$$

- The relative momentum is derived in a relativistic fashion

$$\omega^{fr} = E_f^{fr} - E_i^{fr}$$

$$E_f^{fr} = \sqrt{m_N^2 + [\mathbf{p}^{fr} + \mu/M_X \mathbf{P}_f^{fr}]^2} + \sqrt{M_X^2 + [\mathbf{p}^{fr} - \mu/m_N \mathbf{P}_f^{fr}]^2}$$

- And it is used as input in the non relativistic kinetic energy

$$e_f^{fr} = (p^{fr})^2/(2\mu)$$

- The energy-conserving delta function reads

$$\delta(E_f^{fr} - E_i^{fr} - \omega^{fr}) = \delta(F(e_f^{fr}) - \omega^{fr}) = \left(\frac{\partial F^{fr}}{\partial e_f^{fr}}\right)^{-1} \delta[e_f^{fr} - e_f^{rel}(q^{fr}, \omega^f)]$$

# Relativistic effects in a correlated system

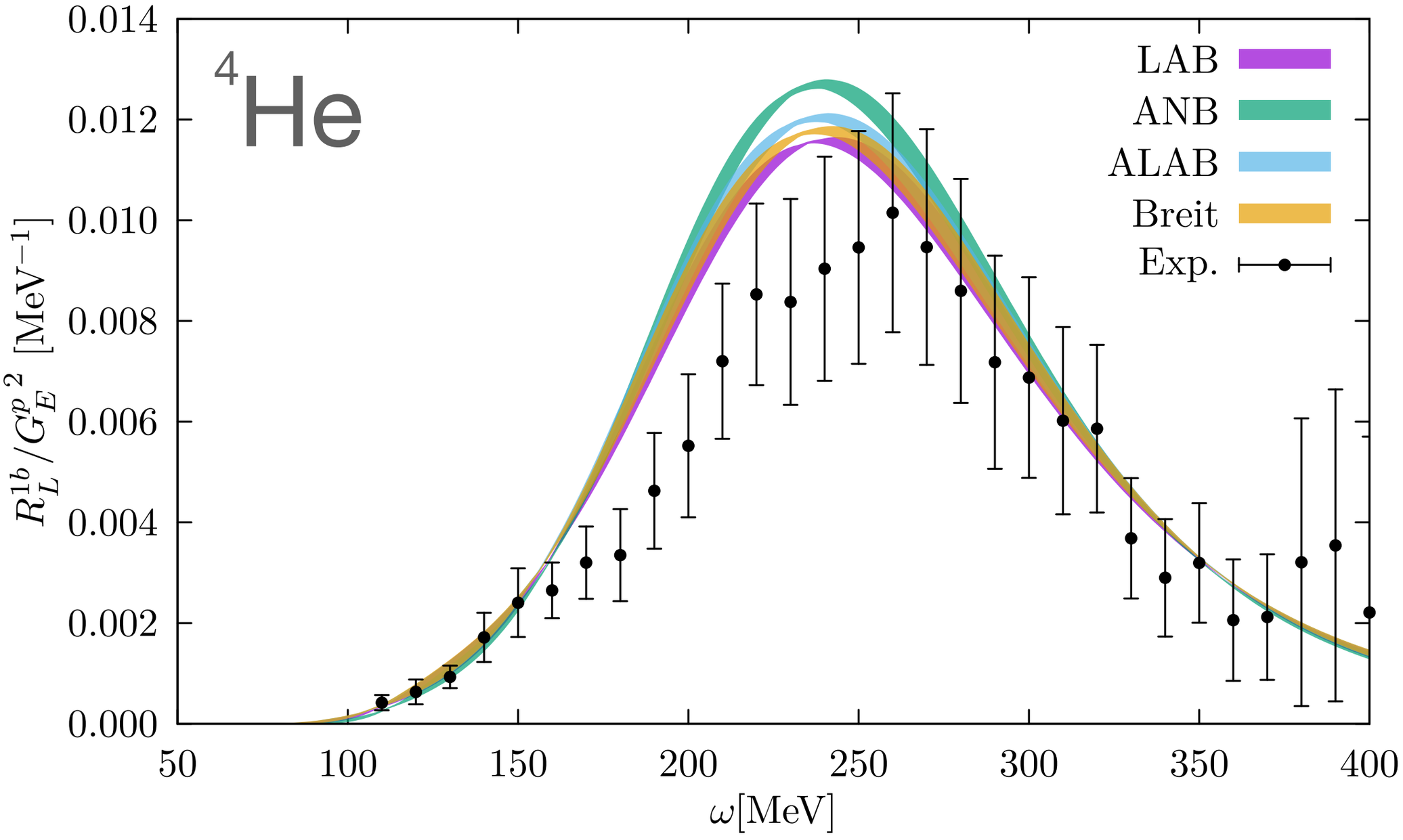


- Longitudinal responses of $^4$He for |q|=700 MeV in the four different reference frames. The different curves are almost identical.

## Extension of the factorization scheme to two-nucleon emission amplitude

$$|X\rangle \longrightarrow |\mathbf{p}\ \mathbf{p}'\rangle \otimes |n_{(A-2)}\rangle = |n_{(A-2)};\mathbf{p}\ \mathbf{p}'\rangle\ ,$$

**We can introduce the two-nucleon Spectral Function...**

$$P(\mathbf{k},\mathbf{k}',E) = \sum_n |\langle n_{(A-2)};\mathbf{k}\ \mathbf{k}'|0\rangle|^2 \delta(E+E_0-E_n)$$

probability of removing two nucleons leaving the A-2 system with energy E

The pure 2-body & the interference contribution to the hadron tensor read

$$W^{\mu\nu}_{2p2h,22} \propto \int d^3k d^3k' d^3p d^3p' \int dE\ P_{2h}(\mathbf{k},\mathbf{k}',E)\langle \mathbf{k}\mathbf{k}'|j^\mu_{12}|\mathbf{p}\mathbf{p}'\rangle\langle \mathbf{p}\mathbf{p}'|j^\nu_{12}|\mathbf{k}\mathbf{k}'\rangle$$

$$W^{\mu\nu}{}_{2p2h,12} \propto \int d^3k\ d^3\xi\ d^3\xi'\ d^3h\ d^3h' d^3p\ d^3p' \phi^{hh'\,*}_{\xi\xi'} \langle \mathbf{p},\mathbf{p}'|j^\nu_{12}|\boldsymbol{\xi},\boldsymbol{\xi}'\rangle$$
$$\left[\Phi^{hh'p'}_k \langle \mathbf{k}|j^\mu_1|\mathbf{p}\rangle + \Phi^{hh'p}_k \langle \mathbf{k}|j^\mu_2|\mathbf{p}'\rangle\right]$$

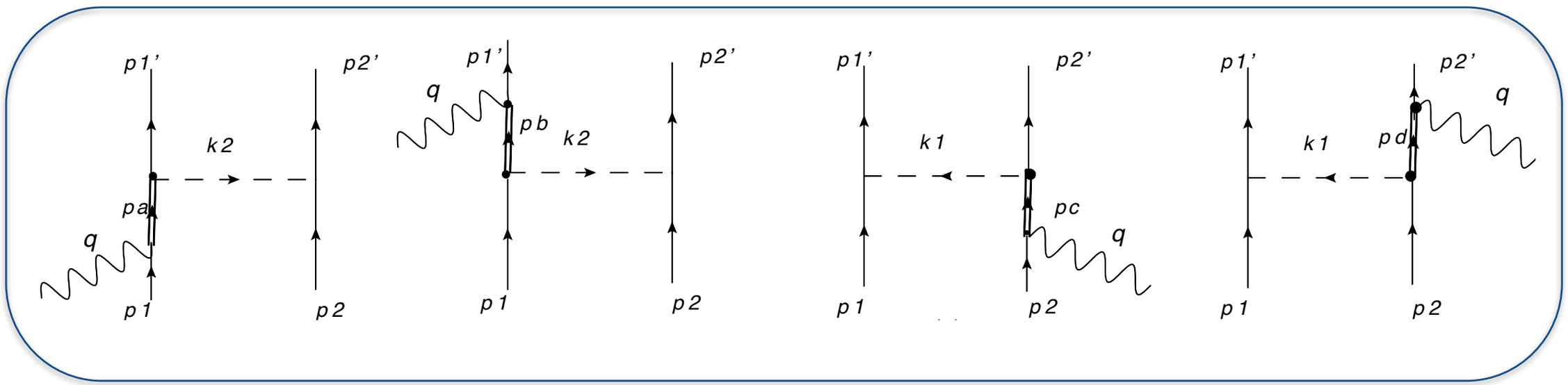


The Rarita-Schwinger (RS) expression for the $\Delta$ propagator reads

$$S^{\beta\gamma}(p, M_\Delta) = \frac{\not{p} + M_\Delta}{p^2 - M_\Delta^2}\left(g^{\beta\gamma} - \frac{\gamma^\beta\gamma^\gamma}{3} - \frac{2p^\beta p^\gamma}{3M_\Delta^2} - \frac{\gamma^\beta p^\gamma - \gamma^\gamma p^\beta}{3M_\Delta}\right)$$

## WARNING

If the condition $p_\Delta^2 > (m_N + m_\pi)^2$ the real resonance mass has to be replaced by $M_\Delta \longrightarrow M_\Delta - i\Gamma(s)/2$ where $\Gamma(s) = \frac{(4f_{\pi N\Delta})^2}{12\pi m_\pi^2}\frac{k^3}{\sqrt{s}}(m_N + E_k)$.

## Hadronic monopole form factors

$$F_{\pi NN}(k^2) = \frac{\Lambda_\pi^2 - m_\pi^2}{\Lambda_\pi^2 - k^2}$$

$$F_{\pi N\Delta}(k^2) = \frac{\Lambda_{\pi N\Delta}^2}{\Lambda_{\pi N\Delta}^2 - k^2}$$

## and the EM ones

$$F_{\gamma NN}(q^2) = \frac{1}{(1 - q^2/\Lambda_D^2)^2} \ ,$$

$$F_{\gamma N\Delta}(q^2) = F_{\gamma NN}(q^2)\Big(1 - \frac{q^2}{\Lambda_2^2}\Big)^{-1/2}\Big(1 - \frac{q^2}{\Lambda_3^2}\Big)^{-1/2}$$

where $\Lambda_\pi = 1300$ MeV, $\Lambda_{\pi N\Delta} = 1150$ MeV, $\Lambda_D^2 = 0.71\mathrm{GeV}^2$, $\Lambda_2 = M + M_\Delta$ and $\Lambda_3^2 = 3.5\ \mathrm{GeV}^2$.